Halophilic mechanisms of the structure, stability, and function of a halophilic dihydrofolate reductase from *Haloarcula japonica* strain TR-1

Yurina Miyashita

Department of Mathematical and Life Sciences,

Graduate School of Science, Hiroshima University

Contents

Abbreviations

CD	Circular dichroism
CSM	Center of spectral mass
DHF	Dihydrofolate
DHFR	Dihydrofolate reductase
EcDHFR	DHFR from *Escherichia coli*
EDTA	Ethylendiaminetetraacetic acid
ESI	Electrospray ionization
HjDHFR	DHFR from *Haloarcula japonica*
HvDHFR	DHFR from *Haloferax volcanii*
IPTG	Isopropyl β-D-thiogalactoside
LB	Luria broth
MES	2-(*N*-morpholino)ethanesulfonic acid
MS	Mass spectrometry
MTE	50 mM 2-(*N*-morpholino)ethanesulfonic acid, 25 mM tris(hydroxymethyl) aminomethane, and 25 mM ethanolamine containing 0.1 mM dithiothreitol and 0.1 mM EDTA (buffer)
MTX	Methotrexate
$NADP^+$	Nicotinamide adenine dinucleotide phosphate (oxidized form)
NADPD	4(R)-^{2}H nicotinamide adenine dinucleotide phosphate (reduced form)
NADPH	Nicotinamide adenine dinucleotide phosphate (reduced form)
NMR	Nuclear magnetic resonance
SDS-PAGE	Sodium dodecyl sulfate-polyacrylamide gel electrophoresis
TDE	20 mM Tris-HCl containing 0.1 mM dithiothreitol and 0.1 mM EDTA (buffer)
THF	Tetrahydrofolate
TMACl	Tetramethylammonium chloride
TMAOH	Tetramethylammonium hydroxide
TME	20 mM Tris-HCl containing 14 mM 2-mercaptoethanol and 0.1 mM EDTA (buffer)

Summary

To elucidate how salt ions affect the structure, stability, and function of enzymes, a novel dihydrofolate reductase (DHFR) from an extremely halophilic archaeon *Haloarcula japonica* strain TR-1 (HjDHFR P1) was overexpressed and purified. Salt concentration dependence of the circular dichroism and fluorescence spectra suggested that the addition of 500 mM NaCl induced structural formation around the substrate-binding site in HjDHFR P1. However, its structural stability for thermal and urea-induced unfolding increased depending on NaCl concentration regardless of this structural change, and the halophilic mechanism of the structural stability is suggested as the contribution of preferential interactions between the protein and salt ions.

On the other hand, HjDHFR P1 showed moderately halophilic characteristics for enzymatic activity at the acidic to neutral pH region, although there are no significant effects of NaCl on its structure. From a comparison of the activation effects of inorganic and organic cations and anions, binding of inorganic anions enhance the enzymatic activity of HjDHFR P1. Furthermore, rapid-phase ligand binding experiments showed that the fluorescence quenching caused by the rapid binding of DHF to HjDHFR P1 increased with increasing NaCl concentration at pH 6.0. In addition, the THF-releasing rate decreased with increasing NaCl concentration, consistent with the decrease of k_{cat} value. These results suggested that the activation mechanism of HjDHFR P1 by salt is via the population change of the anion-unbound and anion-bound conformers, which are binding-incompetent and -competent conformations for DHF, respectively. Conversely, the salt-inactivation mechanism is *via* deceleration of the THF-releasing rate, which is the rate-determining step at the neutral pH region. Such activation mechanisms of structure,

stability, and function may also be possible for other two halophilic DHFRs from *Haloferax volcanii*, and the inactivation mechanism in its function may be a common feature of non-halophilic DHFR from *Escherichia coli*.

Chapter I

Introduction

Salt is the primary component of solutions *in vivo*. Salt ions change the dielectric constant, viscosity, and ionic strength of solutions and are dissolved in cells and blood in living organisms. The salt concentration is maintained at a constant level by several ion channels in biological membranes. It is suggested that salt ions in living organisms play a key role in the stability of biomolecules. For example, nucleic acid has considerable negative charges from rich phosphate groups. Although the repulsive force between these negative charges destabilizes its stereo structure, salt ions stabilize the structure by reducing the repulsive force (Schlick et al. 1994). Although it is not understood clearly how salt ions stabilize or destabilize protein structure, organisms nevertheless employ strategies, such as “salting in” or “salting out”, against high salt concentrations. These effects are related to the reduction of repulsive forces between charged residues on individual protein molecules and preferential interactions between salt ions and proteins (Arakawa and Timasheff 1984).

Recently, much attention has been paid to halophilic proteins, the structures of which are formed and stabilized and the functions of which are activated by the addition of salt, and attempts have been made to elucidate the halophilic mechanisms (Madern et al. 2000, Ortega et al. 2011, Karan and Khare 2011, Ishibashi et al. 2013, Sinha and Khare 2014). Halophilic proteins are found in microorganisms living in saturated salt environments such as salt lakes, salterns, and sometimes commercially distributed natural salts. Since the intracellular salt concentrations of such halophilic microorganisms are identical to the

extracellular conditions to escape osmotic stress, the enzymes they produce have adaptation mechanisms for hypersaline environments (Roesser and Müller 2001). However, the primary and tertiary structures of such halophilic proteins are almost similar to those of non-halophilic homologs produced by organisms living in normal conditions. Although many researchers have suggested the involvement of rich acidic residues in halophilic proteins (Danson and Hough 1997, Mevarech et al. 2000, Oren and Mana 2002, Allers 2010), these studies have not necessarily explained the halophilic mechanism of structure, stability, and function. And it has been unclear how such halophilic enzymes maintain their function under stressful salt conditions.

Dihydrofolate reductase (DHFR) is a famous model enzyme that catalyzes the reduction of dihydrofolate (DHF) to tetrahydrofolate (THF) using nicotinamide adenine dinucleotide phosphate (NADPH) as a coenzyme. It is a ubiquitous enzyme in the cells of all organisms since its product, THF, is essential for the growth and proliferation of cells (Huennekens 1996). DHFR from *Escherichia coli* (EcDHFR) has been investigated widely for its crystal and solution structures (Sawaya and Kraut 1997, Osborne et al. 2003), structural stability (Perry et al. 1987, Garvey and Matthews 1989), folding kinetics (Kuwajima et al. 1991, Jennings et al. 1993), and catalytic mechanism (Fierke et al. 1987, Wang et al. 2014), since it has useful characteristics for a model enzyme such as a relatively small molecular weight of 18 kDa, no disulfide bonds, and existing as a stable monomer (Baccanari et al. 1975, Stone and Morrison 1982, Ohmae et al. 1996, Schnell et al. 2004). The steady-state enzymatic reaction of EcDHFR contains five elementary steps: two binding steps of NADPH and DHF, hydride transfer from NADPH to DHF, and two releasing steps of $NADP^+$ and THF. In addition, the rate-determining step of enzymatic turnover changes from the THF-releasing step at neutral pH to the hydride-

transfer step above pH 8.4 (Fierke at al. 1987). Previously, we reported that EcDHFR lost its activity in a solution containing inorganic cations, such as a potassium phosphate buffer, because they bind to a cation-binding pocket near its Met20 loop (residues 10–24), which is important for its catalytic reaction (Ohmae et al. 2013a).

Many studies have also been performed on the adaptation mechanisms of DHFRs from various environmental bacteria, for example, the moderate thermophile *Geobacillus stearothermophilus* (Guo et al. 2014), hyperthermophile *Thermotoga maritima* (Luk et al. 2014), and piezo-psychrophile *Moritella profunda* (Ohmae et al. 2012, Behiry et al. 2014). Extremely halophile *Haloferax volcanii*. *H. volcanii* was isolated from the Dead Sea, and produces two DHFR enzymes, HvDHFR 1 and 2, whose optimal KCl concentrations for enzymatic activity are more than 3.5 M and 500 mM, respectively (Wright et al. 2002). Studies on HvDHFR 1 have been performed on its X-ray crystal structure (Pieper et al. 1998), solution structure using nuclear magnetic resonance (NMR) (Binbuga et al. 2007, Boroujerdi and Young 2009), structural stability (Wright et al. 2002), folding kinetics (Gloss et al. 2008), and enzymatic function (Zusman et al. 1989, Blecher et al. 1993, Ortenberg et al. 2000). Results of these investigations suggested that destabilization of the unfolded state predominantly invokes the salt-induced stabilization and activation of HvDHFR 1. However, studies on the moderately halophilic enzyme HvDHFR 2 are limited (Ortenberg et al. 2000, Wright et al. 2002), and the mechanisms underlying the optimal salt concentration for its enzymatic activity are still unclear.

Haloarcula japonica strain TR-1 is another extremely halophilic archaeon found in a saltern field at Noto in Japan (Hamamoto et al. 1988). This archaeon requires 41–650 mM Mg^{2+} and high concentrations (1.7–4.3 M) of NaCl for growth and has a morphologically triangular shape (Hamamoto et al. 1988, Nishiyama et al. 1992, Horikoshi et al. 1993,

Takashina et al. 1994). It has been reported that the cell division protein FtsZ1, α-amylase, and pyrophosphatase from this archaeon show halophilic characteristics (Ozawa et al. 2005, Onodera et al. 2013, Wakai et al. 2013). Therefore, we have used DHFR from *H. japonica* (HjDHFR) as a halophilic model protein. *H. japonica* strain TR-1 has three DHFR genes, *folA1*, *folA2*, and *folA3*, encoded on chromosome 1 (C1), chromosome 2 (C2), and plasmid 1 (P1), respectively, in its genome, which consists of five replicons (Nakamura et al. 2011). The nucleotide sequences of these genes are registered in the GenBank/EMBL/DDBJ sequence database under the accession numbers AB986556, AB986557, and AB986558, respectively. Among the three DHFRs, HjDHFR P1 has a highly homologous amino acid sequence to EcDHFR, approximately 47.5% (Fig. I-1), and the SWISS-MODEL server (http://swissmodel.expasy.org/) predicted an almost identical stereo structure (Fig. I-2). However, the composition of acidic residues (13.3%) is lower than that of EcDHFR (15.7%), contrary to the traditional hypothesis.

Considering such research backgrounds, the purposes of this study were set to elucidate the effects of salt on the structure, stability, and function of HjDHFR P1, and discuss the halophilic mechanisms shown by this enzyme. I evaluated the effects of salt on the structure using circular dichroism (CD) and fluorescence spectra, on the structural stability by thermal unfolding and urea-induced unfolding, and on the elementary steps in the catalytic cycle by monitoring the pH- and salt concentration-dependences of its enzyme activity, deuterium isotope effects, and rapid-phase ligand binding kinetics using stopped-flow fluorescence quenching. On the basis of the results of these experiments, I discussed the activation and inactivation mechanisms of HjDHFR P1 by salt and compared the effects of salt with other halophilic DHFRs, namely, HvDHFR 1 and 2, and non-halophilic EcDHFR.

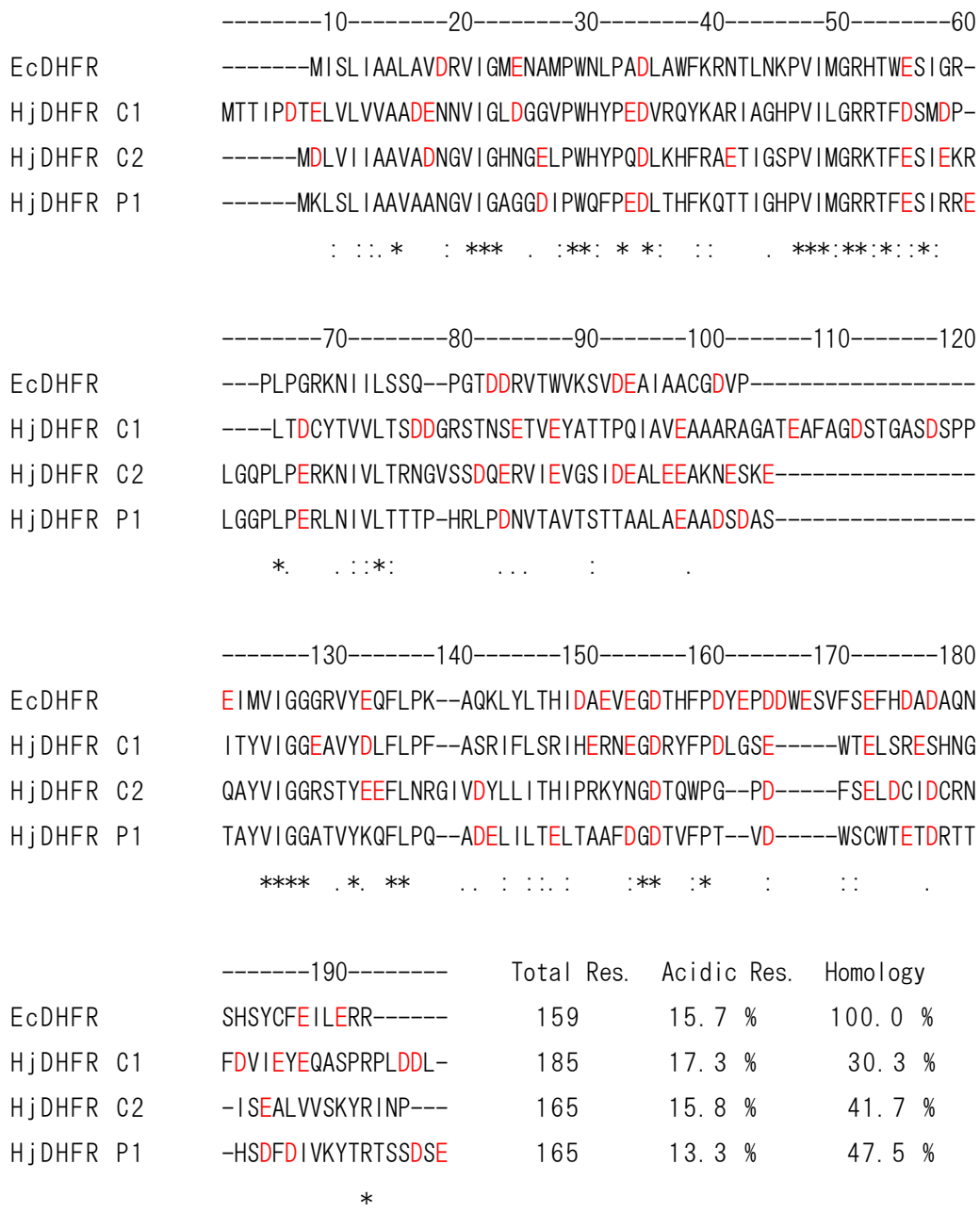

Fig. I-1. Amino acid sequences of EcDHFR and three DHFRs (C1, C2, and P1) from *H. japonica* strain TR-1. Multiple alignments were conducted by the CLUSTALW program on a DNA Data Bank of Japan server (http://www.ddbj.nig.ac.jp/). The symbols "*", ":", and "." below the alignment indicate fully, strongly, and weakly conserved residues, respectively. Acidic amino acid residues are indicated by red letters. Sequence length, ratio of acidic residues, and homology levels to EcDHFR are also indicated at the end of each sequence.

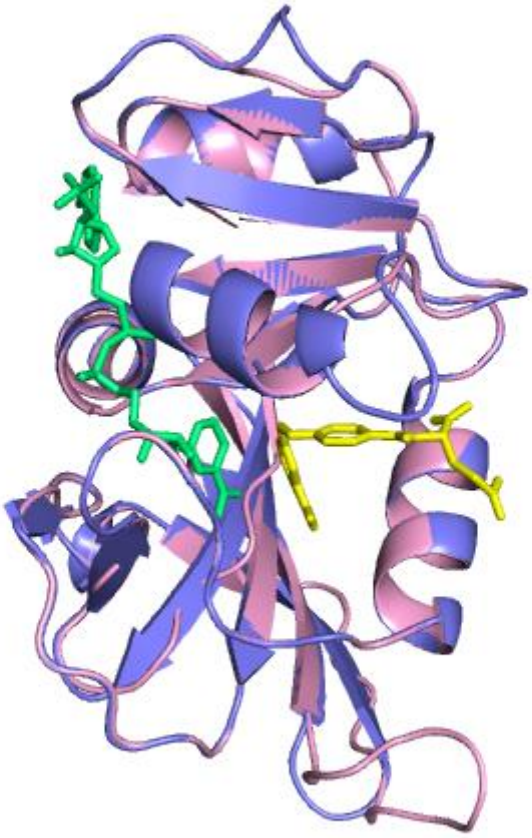

Fig. I-2. Superimposed drawing of the backbone structures of the EcDHFR crystal structure (PDB code: 1rx2; pink) and the structure of HjDHFR P1 (blue) predicted by the SWISS-MODEL server (http://swissmodel.expasy.org/). NADPH (green) and folate (yellow) bound to EcDHFR are drawn as a stick model. The figure was prepared using the PyMol program (http://www.pymol.org/).

Chapter II

Materials and Methods

II-1. Construction of overexpression plasmids for HjDHFRs

Genomic DNA of *H. japonica* strain TR-1 was prepared according to the method of Takashina *et al.* (Takashina et al. 1990), and presented from Prof. K. Nakasone of Kinki University. The DNA sequences of the synthesized primers used in this study are indicated in Table II-1.

DNA fragments encoding the *folA1*, *folA2*, and *folA3* genes were amplified by PCR using KOD-plus DNA polymerase (TOYOBO, Osaka, Japan) and appropriate primers. The amplified DNA fragments were purified by a Wizard SV Gel and PCR Clean-Up System (Promega, Madison, WI), ligated to *Sma*I-digested pUC118 vector using a T4 DNA ligase (NEW ENGLAND BioLabs, Ipswich, MA), and transformed into *E. coli* HB101 competent cells (Takara Bio, Otsu, Japan). Cultures were grown at 37°C for 60 h on a Luria broth (LB) plate containing 200 μg/mL ampicillin and 20 μg/mL trimethoprim. The overexpression of the HjDHFR proteins in *E. coli* cells was confirmed by sodium dodecyl sulfate-polyacrylamide gel electrophoresis (SDS-PAGE) after 60 h cultivation in LB liquid medium containing 100 μg/mL ampicillin and 20 μg/mL trimethoprim. Then, the plasmids were extracted by a PureYield Plasmid Miniprep System (Promega) and the DNA sequences of the HjDHFR genes were confirmed by a CEQ8000 gene analysis system (Beckman Coulter, Brea, CA).

Since HjDHFR C1 and C2 proteins could not be overexpressed in *E. coli* cells, we then used a pET expression system. The *folA1* and *folA2* genes were amplified and purified by the same methods described above, except for using newly-synthesized 5′

primers and ligation to a *Sma*I-digested pHSG398 vector (Takara Bio). The ligated plasmids were transformed into *E. coli* DH5α competent cells (Takara Bio) and the transformants were cultured on an LB plate containing 20 μg/mL chloramphenicol, 50 μg/mL isopropyl β-D-thiogalactoside (IPTG), and 50 μg/mL 5-bromo-4-chloro-3-indolyl-β-D-galactoside. Transformants containing the plasmids encoding the HjDHFR genes were selected as white-colored colonies. Purified plasmids were digested with *Nde*I and *Eco*RI, and ligated to the pET21a vector (Merck, Darmstadt, Germany) digested with the same restriction enzymes. The ligated plasmids were transformed into *E. coli* DH5α competent cells and the transformants were cultured on an LB plate containing 200 μg/mL ampicillin. Plasmids encoding the HjDHFR genes were selected by a colony-directed PCR method using GoTaq DNA polymerase (Promega), and purified plasmids were transformed into *E. coli* BL21 (DE3) competent cells (Merck). Cultures were grown at 37°C for 8 h in LB liquid medium containing 100 μg/mL ampicillin, and the expression of the HjDHFR proteins was induced by adding IPTG at a final concentration of 0.1 mM to the culture. After cultivation for an additional 16 h, the overexpression of the HjDHFR proteins was confirmed by SDS-PAGE. The DNA sequences of the HjDHFR genes were also confirmed by the CEQ8000 system.

As the HjDHFR C1 protein could not be overexpressed by using the pET expression system, we used the pCold expression system. The *folA1* gene was transferred from the pHSG398-based plasmid to the pCold IV vector (Takara Bio), transformed into *E. coli* DH5α competent cells, and the plasmid was selected as described above. The transformants were grown at 37°C for 8 h in LB liquid medium containing 100 μg/mL ampicillin, and the expression of the HjDHFR C1 protein was induced by the addition of 0.1 mM IPTG and lowering the temperature to 16°C. After an additional 16 h culture,

proteins in *E. coli* cells were confirmed by SDS-PAGE, and the DNA sequence was also confirmed by the CEQ8000 system.

II-2. Purification of HjDHFR P1 protein

E. coli strain HB101 containing the HjDHFR P1 overexpression plasmid was grown at 37°C for 60 h in LB liquid medium containing 100 μg/mL ampicillin and 20 μg/mL trimethoprim. The cells were harvested by centrifugation, resuspended in 20 mM Tris-HCl (pH 8.0) containing 14 mM 2-mercaptoethanol and 0.1 mM EDTA (TME buffer), and disrupted by sonication. After removing the cell debris by centrifugation at 4°C, 31,000 ×*g*, and 30 min, streptomycin sulfate at a final concentration of 2% (wt/vol) was added to the solution and mixed mildly for 30 min at 4°C. The soluble fraction was collected by centrifugation at 4°C, 13,000 ×*g*, and 20 min, and loaded on an affinity column packed with methotrexate-agarose resin (Sigma-Aldrich, St. Louis, MO). The column was washed with TME buffer containing 500 mM NaCl, and HjDHFR P1 protein was eluted in a 0.1 M NaOH solution. To avoid modification or degradation of the protein, the eluted solution was poured directly into a beaker containing a 1 M Tris-HCl solution (pH 8.0). Then, the eluted solution was dialyzed against TME buffer and concentrated using a small DE52 column (GE Healthcare UK Ltd., Buckinghamshire, UK). To remove the remaining ligands perfectly, the protein was fully unfolded by dialyses against TME buffer containing 3 M guanidine hydrochloride and refolded by dialyses against 20 mM Tris-HCl (pH 8.0) containing 0.1 mM dithiothreitol and 0.1 mM EDTA (TDE buffer). The concentration of the purified protein was determined by a molar extinct coefficient of 20,910 $M^{-1} \cdot cm^{-1}$ at 280 nm, which was calculated from the amino acid composition.

II-3. Identification of molecular weight by mass spectrometry

Purified HjDHFR P1 protein was verified by electro-spray ionization (ESI) mass spectrometry (MS) using an LTQ Orbitrap XL system (Thermo Fisher Scientific, Waltham, MA). The solvent for ESI was 50% acetonitrile and 50% water containing 0.1% formic acid. The protein concentration was approximately 20 μM.

To check the mass of the trypsin-digested fragments, approximately 200 μg/mL (at the final concentration) trypsin was added to the protein solution and reacted at 37°C. Aliquots of the reaction mixture were taken at 0, 0.5, 1, 2, 4, 8, and 24 h after the digestion reaction was initiated, and diluted with the solvent for ESI to stop the reaction. The amino acid sequence of the N-terminus fragment was determined by tandem mass (MS/MS) spectra.

II-4. Circular dichroism spectra

Far-ultraviolet circular dichroism (CD) spectra of the HjDHFR P1 protein were measured using a J-720W spectropolarimeter (Jasco, Inc., Tokyo, Japan) as described previously (Ohmae et al. 2005). The temperature was maintained at 25°C by a Peltier-controlled thermobath (PTC-348W; Jasco, Inc.). The solvent used was TDE buffer (pH 8.0) or 25 mM 2-(N-morpholino)ethanesulfonic acid (MES), 12.5 mM Tris, and 12.5 mM ethanolamine buffer containing 0.05 mM dithiothreitol and 0.05 mM EDTA, whose pH was adjusted to 6.0 by acetic acid. The protein concentration was approximately 10 μM with an optic cell with a light path of 1 mm. When the CD spectra of the HjDHFR P1–folate and HjDHFR P1–NADPH binary complexes were measured, the samples were equilibrated for 30 min at 25°C after adding the ligands, and the CD spectrum of the same concentration of ligand was subtracted from that of the binary complex, because both

ligands showed obvious CD spectra. The concentrations of folic acid and NADPH (Oriental Yeast, Tokyo, Japan) were determined spectrophotometrically using molar extinction coefficients of 27,000 $M^{-1}\cdot cm^{-1}$ at 282 nm and 6,200 $M^{-1}\cdot cm^{-1}$ at 339 nm, respectively.

II-5. Fluorescence spectra

Fluorescence spectra of the HjDHFR P1 protein were measured using an FP-750 spectrofluorometer (Jasco, Inc.) as described previously (Ohmae et al. 2005). The excitation and emission wavelengths were set at 290 and 300−450 nm, respectively. The temperature was maintained at 25°C using a circulating thermobath (NESLAB RTE-110; Thermo Fischer Scientific). The solvent used was 50 mM MES, 25 mM Tris, and 25 mM ethanolamine buffer containing 0.1 mM dithiothreitol and 0.1 mM EDTA (MTE buffer), whose pH was adjusted to 8.0 by tetramethylammonium hydroxide (TMAOH). The protein concentration was 1−2 μM. The samples were equilibrated for 30 min at 25°C after adding salt. The center of fluorescence spectral mass (CSM) was calculated from the obtained spectra using the following equation:

$$\mathrm{CSM} = \frac{\sum(\nu_i \ F_i)}{\sum F_i} \qquad (\mathrm{II}-1)$$

where ν_i and F_i are wavenumber (cm^{-1}) and fluorescence intensity at the wavelength i, respectively.

II-6. Equilibrium dissociation constants

The equilibrium dissociation constant between the HjDHFR P1 protein and ligands (folate or NADPH) was measured using fluorescence-quenching of the intrinsic tryptophan residues by the binding of ligands, as described previously (Ohmae et al. 2005).

The excitation and emission wavelengths were 290 and 300−550 nm, respectively. The solvent used was MTE buffer whose pH was adjusted to 8.0 with TMAOH. The protein concentration was approximately 20 μM. The samples were equilibrated for 30 min at 25°C before the fluorescence spectra were measured. The observed fluorescence intensity at 346 nm, F, was analyzed by the following equation using a nonlinear least-squares analysis with an Origin program (Origin Lab., Northampton, MA):

$$F = F_0[\mathrm{P}]_\mathrm{t} + \frac{\Delta F}{2}\left\{(K_\mathrm{d} + [\mathrm{P}]_\mathrm{t} + [\mathrm{L}]_\mathrm{t}) - \sqrt{(K_\mathrm{d} + [\mathrm{P}]_\mathrm{t} + [\mathrm{L}]_\mathrm{t})^2 - 4[\mathrm{P}]_\mathrm{t}[\mathrm{L}]_\mathrm{t}}\right\} \quad (\mathrm{II}-2)$$

where F_0 is the molar fluorescence intensity without ligands, ΔF is the molar fluorescence intensity change between the protein-ligand complex and the free protein, K_d is the dissociation constant, and $[\mathrm{P}]_\mathrm{t}$ and $[\mathrm{L}]_\mathrm{t}$ are the concentrations of the protein and ligand, respectively. The concentration of L-Tryptophan (Wako Pure Chemical Industries, Ltd., Osaka, Japan) was determined spectrometrically using molar extinction coefficients of 5,579 $\mathrm{M^{-1}cm^{-1}}$ at 278 nm.

II-7. Thermal unfolding

Thermal unfolding of the HjDHFR P1 protein was monitored by molar ellipticity at 222 nm, $[\theta]_{222}$, under 0−1,000 mM NaCl concentration. The temperature was increased from 5 to 80°C at a rate of 45°C·$\mathrm{h^{-1}}$, and monitored by a thermosensor inserted into the sample solution. The solvent used was TDE buffer (pH 8.0). The protein concentration was 1.5−2 μM in an optic cell with a light path of 10 mm. The reversibility of unfolding was checked by CD spectra at 10°C before and at 30 min after the unfolding measurement. The results were analyzed by a nonlinear least-squares analysis using the following equation (Ohmae et al. 2005):

$$[\theta]_{222} = \frac{[\theta]_{\mathrm{N}} + [\theta]_{\mathrm{U}} \exp(-\Delta G_{\mathrm{u}}/RT)}{1 + \exp(-\Delta G_{\mathrm{u}}/RT)} \qquad (\mathrm{II}-3)$$

where ΔG_{u} is the change in Gibbs free energy with unfolding, R is the gas constant, T is the absolute temperature, and $[\theta]_{\mathrm{N}}$ and $[\theta]_{\mathrm{U}}$ are the molar ellipticities at native and unfolded states, respectively, which are estimated by assuming linear temperature dependency. The temperature dependence of ΔG_{u} was calculated using the following equation:

$$\Delta G_{\mathrm{u}} = \Delta H_m + \Delta C_{\mathrm{P}}(T - T_{\mathrm{m}}) - T\left\{\frac{\Delta H_{\mathrm{m}}}{T_{\mathrm{m}}} + \Delta C_{\mathrm{P}} \ln\left(\frac{T}{T_{\mathrm{m}}}\right)\right\} \qquad (\mathrm{II}-4)$$

where T_{m} is the midpoint temperature of the transition, ΔH_{m} is the change in enthalpy with unfolding at T_{m}, and ΔC_{p} is the change in heat capacity, which is assumed to be independent of temperature in the experimental range.

II-8. Urea-induced unfolding

Urea (ultra-pure product from MP Biomedicals, Solon, OH) -induced unfolding of HjDHFR P1 protein was monitored by fluorescence spectra at 25°C. The solvent used was TDE buffer (pH 8.0). The protein concentration was 1 μM. The samples were equilibrated for 16 h before spectral measurement. Thirty concentrations of urea were used for each NaCl concentration (0, 250, 500, 750, and 1,000 mM). Calculated CSM values using eq. II-1 were analyzed by eq. II-3 using a nonlinear least-squares analysis with the substitution of $[\theta]_{222}$, $[\theta]_{\mathrm{N}}$, and $[\theta]_{\mathrm{U}}$ with $\mathrm{CSM}_{\mathrm{obs}}$, $\mathrm{CSM}_{\mathrm{N}}$, and $\mathrm{CSM}_{\mathrm{U}}$, respectively. The urea-concentration dependence of ΔG_{u} was assumed as follows (Pace 1985):

$$\Delta G_{\mathrm{u}} = \Delta G_{\mathrm{u}}^{\mathrm{o}} - m[\mathrm{urea}] \qquad (\mathrm{II}-5)$$

where $\Delta G^{\circ}{}_{\mathrm{u}}$ is the change in Gibbs free energy without urea and m is the parameter reflecting the cooperativity of unfolding. The midpoint urea concentration of unfolding,

$\Delta G_u = 0$, was defined as C_m.

II-9. Enzyme assay

The enzymatic activity of HjDHFR P1 was measured using a V-560 spectrophotometer (Jasco, Inc.). Temperature was maintained at 25°C with a circulating thermobath (NESLAB RTE-5; Thermo Fisher Scientific). The solvent used was MTE buffer. The pH of the buffer was modulated by TMAOH or acetic acid. The concentrations of DHF (Sigma-Aldrich) and NADPH were determined spectrophotometrically using molar extinction coefficients of 28,400 $M^{-1}\cdot cm^{-1}$ at 282 nm and 6,200 $M^{-1}\cdot cm^{-1}$ at 339 nm, respectively. The initial velocity (V) of the reaction was determined using a differential molar extinction coefficient of 11,800 $M^{-1}\cdot cm^{-1}$ at 340 nm (Fierke et al. 1987).

II-9-1. pH dependence of enzyme activity

pH dependence of the HjDHFR P1 activity was measured under 0, 200, and 1,000 mM NaCl concentrations. The reaction solution without DHF was pre-incubated for 10 min at 25°C, and the reaction was initiated by the addition of the DHF solution, which was also pre-incubated at 25°C. The concentrations of the enzyme, NADPH, and DHF in the reaction mixture were 0.08, 50, and 50 μM, respectively. Observed initial velocity, V, was plotted against pH and fitted to the following equation (Stone and Morrison 1984):

$$V = \frac{V_i}{1 + \frac{[H^+]}{K_a} + \frac{K_b}{[H^+]}} \qquad (II-6)$$

where V_i is the pH-independent velocity, K_a and K_b are acid dissociation constants, and $[H^+]$ is proton concentration.

II-9-2. Effects of salt on enzyme activity

The effects of NaCl, tetramethylammonium chloride (TMACl), and sodium acetate (CH_3COONa) concentrations on the enzyme activity of HjDHFR P1 were measured at 25°C and pH 8.0. The effect of NaCl concentration was also measured at pH 6.0 and 10.0. The concentrations of the enzyme, NADPH, and DHF were the same as for the pH-dependence measurements. The initiating method of the reaction was also the same as for the pH-dependence measurements.

II-9-3. Deuterium isotope effects on steady-state kinetics

4(R)-^{2}H reduced NADPH (NADPD) was synthesized from $NADP^+$ (Oriental Yeast) and 2-propanol-d_8 (Sigma-Aldrich) by the catalytic reaction of alcohol dehydrogenase from *Thermoanaerobium brockii* (Sigma-Aldrich) as reported previously (Chen et al. 1987). Synthesized NADPD was purified using AG MP-1 anion exchange resin (BIO-RAD, Hercules, CA) by the method of Viola et al. (1979), and stored at –20°C. Just before use, NADPD was thawed and desalted by a HiTrap desalting column (GE Healthcare Japan, Tokyo, Japan), and its purity and concentration were confirmed by absorptions at 260 and 340 nm. NADPH used in this experiment was also prepared by the same method to normalize the effects of contaminating salt ions. The deuterium isotope effect in the steady-state catalytic reaction, ${}^{D}V$, was evaluated as follows (David et al. 1992):

$$ {}^{D}V = \frac{V_{\mathrm{NADPH}}}{V_{\mathrm{NADPD}}} \qquad (\mathrm{II}-7) $$

where V_{NADPH} and V_{NADPD} are the initial velocities of the enzymatic reaction using NADPH and NADPD as a cofactor, respectively. The concentrations of the enzyme, cofactors, and DHF were the same as for the pH-dependence measurements.

II-9-4. Steady-state enzyme kinetics

Steady-state enzyme kinetics were measured at 25°C and pH 6.0 or 8.0. When the kinetics parameters for DHF were measured, the concentration of DHF was varied from 0 to 100 μM, employing 50 μM NADPH. When those for NADPH were measured, the concentration of NADPH was varied from 0 to 150 μM, employing 50 μM DHF. Enzyme concentrations were 10 to 200 nM, depending on the pH and NaCl concentration, and determined by a methotrexate (MTX) titration method (Williams et al. 1979). Reaction solutions without DHF or NADPH were pre-incubated for 10 min before initiating the reaction by the addition of the pre-incubated the other substrate solution.

II-9-5. Effects of NaCl concentration during pre-incubation

The effects of NaCl concentration during pre-incubation were measured at 25°C and pH 6.0. The final concentrations of the enzyme, NADPH, and DHF were the same as for the pH-dependence measurements. Enzyme and NADPH or DHF were pre-incubated for 10 min under 0 to 2,000 mM NaCl, and 100 μL of the solution were added to 900 μL of the pre-incubated substrate solution containing an appropriate concentration of NaCl for a final concentration of 500 mM. Reaction rate was calculated from absorption change from 60 to 90 s, since that from 0 to 60 s was nonlinear for several conditions. Then, it was plotted against NaCl concentration during pre-incubation, and fitted to the following equation:

$$V = \frac{V_{\max}[\mathrm{NaCl}]}{K_{\mathrm{d}} + [\mathrm{NaCl}]} + V_0 \qquad (\mathrm{II}-8)$$

where $V_{\max}$ is the maximum velocity, K_{d} is the dissociation constant between enzyme and salt, [NaCl] is the NaCl concentration, and V_0 is the NaCl concentration-independent velocity, which is need to correct the effects of 500 mM NaCl included in the reaction

mixture.

II-10. Rapid-phase ligand binding kinetics

The rapid-phase ligand binding kinetics of DHF and NADPH to HjDHFR P1 at various NaCl concentrations were measured by a fluorescence quenching method using a model SX20 stopped-flow system (Applied Photophysics, Surrey, UK). Three intrinsic tryptophan side chains were excited at 280 nm, and fluorescence at around 350 nm was detected using a V-350 bandpass filter (Hokushin Optical Works Ltd., Tokyo, Japan). The buffer used was MTE buffer (pH 6.0) and temperature was maintained at 24.5°C. The final concentrations of the enzyme, DHF, and NADPH in the reaction mixture were 4.8, 50, and 25 μM, respectively. The resulting fluorescence intensity as a function of time, $F(t)$, was fitted to a single exponential with linear decay:

$$F(t) = A\exp(k_{\mathrm{app}}t) + k_{\mathrm{lin}}t + F_{\infty} \qquad (\mathrm{II}-9)$$

where A, k_{app}, k_{lin}, and F_{∞} are the amplitude of fluorescence quenching, apparent rate constants for the exponential and linear phases, and finally attaining fluorescence intensity, respectively. Since the obtained k_{lin} values were negligibly small for the DHF-binding measurements, fitting was repeated with this parameter fixed to zero.

To determine ligand-association and -dissociation rate constants, the concentration of HjDHFR P1 was reduced to 1 μM and those of the ligands were varied from 10 to 50 μM. Then, the fluorescence decay data were fitted to eq. II-9, and the obtained k_{app} was fitted to the following equation (Grubbs et al. 2011):

$$k_{\mathrm{app}} = k_{\mathrm{on}}[\mathrm{ligand}] + k_{\mathrm{off}} \qquad (\mathrm{II}-10)$$

where k_{on} and k_{off} are the association and dissociation rate constants, respectively, and [ligand] indicates ligand concentration. The rate constants for THF were measured at pH

8.0, and the k_{lin} parameter was fixed to zero once again for the THF-binding measurements.

Table II-1. Oligonucleotide primers used in the PCR amplification of DHFR genes from *H. japonica*.

Primer	Sequence
C1-pUC-F	5′-AGGAACTTCCATGACGACGATACCCGATAC-3′
C1-pUC-R	5′-GAGGATCCTCAGAGGTCGTCGAGCGGTCGC-3′
C2-pUC-F	5′-AGGAACTTCCATGGACCTCGTAATTATCGC-3′
C2-pUC-R	5′-GAGGATCCCTACGGGTTGATCCTGTATTTT-3′
P1-pUC-F	5′-AGGAACTTCCATGAAACTCTCGCTGATCGC-3′
P1-pUC-R	5′-GAGGATCCTCATTCCGAGTCACTGCTGGTT-3′
C1-pET-F	5′-GGCATATGACGACGATACCCGATACCGAAC-3′
C2-pET-F	5′-GGCATATGGACCTCGTAATTATCGCTGCAG-3′

Chapter III

Results

III-1. Construction of overexpression plasmids and protein purification

III-1-1. Construction of overexpression plasmids for HjDHFRs

I tried to construct overexpression plasmids for all three DHFR genes from *H. japonica* strain TR-1. However, only HjDHFR P1 could be overexpressed in *E. coli* cells by a conventional cloning method. Although HjDHFR C2 could be overexpressed as inclusion bodies when the vector was changed to pET21a, HjDHFR C1 could not be overexpressed by either pET21a or pCold IV vectors (Fig. III-1). Mevarech and colleagues reported previously that another extremely halophilic archaeon, *Haloferax volcanii*, has two DHFRs, HvDHFR 1 and HvDHFR 2, and the former goes to the insoluble fractions, while the latter goes to the soluble fractions when they are overexpressed in *E. coli* (Blecher et al. 1993, Ortenberg et al. 2000). Therefore, HjDHFR C2 and P1 corresponded to HvDHFR 1 and 2, respectively, although both HjDHFRs have higher sequence homology to HvDHFR 1 than HvDHFR 2. As mentioned below, HjDHFR P1 also has considerable similarity to HvDHFR 2 in its functional characteristics.

Conversely, Ortenberg et al. (2000) reported that an *H. volcanii* mutant, in which both HvDHFR genes were deleted, could grow in minimal medium only when it was supplemented with the essential components for growth without DHFR, thymidine, glycine, methionine, pantothenic acid, and hypoxanthine. Thus, the third DHFR would not exist in *H. volcanii*, and HjDHFR C1 may have unique characteristics. However, I can't check it until the enzyme is purified from the original bacterium or a successful

expression system of the recombinant protein is constructed.

III-1-2. Purification of HjDHFR P1 protein

The overexpression of HjDHFR P1 protein in *E. coli* cells and its purification as a prominent band were also confirmed by SDS-PAGE (Fig. III-1). However, the mass weight of the purified protein measured by ESI-MS was 1,306 Da bigger than the value calculated from its amino acid composition. To clarify the discrepancy of both values, the mass of trypsin-digested fragments was measured. As a result, the mass of the N-terminus fragment was 1,306 Da bigger than the theoretical value due to the presence of an additional 13 residues (TMITNSSSVPGTS) from the *lacZ′* gene encoded by the pUC118 vector with acetylation of the N-terminus threonine, which was elucidated by MS/MS (Fig. III-2). As Murakami et al. (2010, 2011) reported previously, purified DHFRs from deep-sea bacteria showed piezophilic characteristics and not halophilic ones, although they had the same additional residues as HjDHFR P1 at their N-terminus. Therefore, the halophilic properties of HjDHFR P1 described in this thesis are not derived from these additional residues.

III-2. Effects of salt on the structure and stability of HjDHFR P1

III-2-1. Effects of salt on secondary structure

Fig. III-3A shows NaCl concentration dependence of the CD spectra of HjDHFR P1 protein at 25°C and pH 8.0. The CD spectrum of HjDHFR P1 had a negative peak of –8,760 deg·cm^2·dmol^{-1} at 202 nm in the absence of NaCl. As the NaCl concentration was increased to 500 mM, the peak wavelength shifted to 215 nm with a decrease in molar ellipticity at 222 nm from –4,110 to –5,960 deg·cm^2·dmol^{-1}. The isoelliptic point

observed at 210 nm suggested the existence of two structural states. These results indicated that the increase of NaCl concentration induced considerable secondary structure formation in HjDHFR P1, since the negative ellipticity at 222 nm mainly represents an n-π* transition of the amide backbone, which forms α-helices (Holzwarth and Doty 1965, Woody 1977).

Conversely, the CD spectrum of HjDHFR P1 at pH 6.0 in the absence of NaCl was almost similar to that at pH 8.0 in the presence of 500 mM NaCl, although the spectrum was still changed slightly by the addition of NaCl with an isoelliptic point at 210 nm (Fig. III-3B). This result suggested that the secondary structure of HjDHFR P1 was already formed at pH 6.0 in the absence of NaCl, although the addition of NaCl still caused small structural changes.

III-2-2. Effects of salt on tertiary structure

To confirm the tertiary structure surrounding the three tryptophan residues of HjDHFR P1, the NaCl concentration dependence of the fluorescence spectra was measured at 25°C and pH 8.0 (Fig. III-4A). The peak wavelength of the HjDHFR P1 fluorescence spectrum in the absence of NaCl, 346 nm, was shifted to 342 nm by adding 500 mM NaCl. This result suggested the formation of a tertiary structure of HjDHFR P1 surrounding the tryptophan residues, since the blue shift of peak wavelength in the fluorescence spectra reflects the screening of the internal tryptophan side chains from the solvent.

In addition, the calculated CSM value of each fluorescence spectrum using eq. II-1 increased significantly from 0 to 500 mM NaCl, and increased moderately above 500 mM (Fig. III-4B). Similarly, the molar ellipticity at 222 nm decreased significantly below 500

mM NaCl, and remained almost constant above 500 mM, as also shown in Fig. III-4B. Such spectral changes were also reported for other halophilic DHFRs from *H. volcanii* (Wright et al. 2002). These results indicated that the structure of HjDHFR P1 changed significantly from 0 to 500 mM NaCl, and the linear increase of the CSM values above 500 mM would reflect not structural change but the NaCl dependence of tryptophan fluorescence itself.

III-2-3. Effects of salt on ligand binding

To examine the effects of salt on ligand binding, I measured the folate and NADPH concentration dependence of the fluorescence spectra at 25°C and pH 8.0 under various NaCl concentrations. As shown in Fig. III-5A, folate concentration dependence of the fluorescence intensity of HjDHFR P1 at 346 nm agreed with that of L-tryptophan at all examined NaCl concentrations, suggesting a difficulty in calculation of K_d values by this method. Conversely, NADPH concentration dependence of the fluorescence intensity was slightly changed by the addition of NaCl (Fig. III-5B). From the change of peak intensity, the equilibrium dissociation constant, K_d, between HjDHFR P1 and NADPH was calculated according to the one-to-one binding model (eq. II-2). The obtained K_d value in the absence of NaCl, 33.7 ± 9.6 μM, was independent of the NaCl concentration (Table III-1). The binding for NADPH was also confirmed by the change of molar ellipticity at 222 nm in the absence of NaCl at pH 8.0. The obtained K_d value was 19.5 ± 20.7 μM, which was coincident with the value obtained from the fluorescence measurement (Fig. III-5B and Table III-1). Wright et al. (2002) reported that the K_d values of HvDHFR 2 for DHF and NADPH at 0.5−1.0 M KCl were 17−18 μM and approximate 30 μM, respectively, and almost independent of salt concentration, although those of HvDHFR 1

depended significantly on the salt concentration. Therefore, HjDHFR P1 has similar affinity to HvDHFR 2 for cofactor, and also has a similar salt concentration-independent K_d value, in addition to the same overexpression pattern in *E. coli* described above.

To confirm the structural changes induced by ligand binding, the folate and NADPH concentration dependence of the CD spectra of HjDHFR P1 was measured at 0 and 500 mM NaCl. As shown in Fig. III-6A and III-6B, the addition of folate had no effect on the CD spectra of HjDHFR P1 in the absence or presence of NaCl. Conversely, the addition of NADPH had different effects on the CD spectra; the NADPH concentration-dependent spectral change was observed from 0 to 300 μM in the absence of NaCl (Fig. III-6C), although the spectra almost overlapped at all NADPH concentrations in the presence of NaCl (Fig. III-6D). The CD spectrum of HjDHFR P1 with 300 μM NADPH in the absence of NaCl almost overlapped that observed without NADPH in the presence of 500 mM NaCl. This result suggested that the binding of NADPH induced a similar structural change to HjDHFR P1 as the addition of NaCl.

III-2-4. Effects of salt on thermal unfolding

To examine the effects of salt on structural stability, I monitored the thermal unfolding of HjDHFR P1 by the molar ellipticity change at 222 nm from 0 to 1,000 mM NaCl (Fig. III-7A). In the absence of NaCl, the negative molar ellipticity of HjDHFR P1 decreased monotonously from 5 to 35°C and then decreased slightly at higher temperatures in a linear fashion. This monotonous decrease of molar ellipticity was also observed at the low temperature region of 5–20°C at 100, 150, and 200 mM NaCl. These decreases of molar ellipticity would reflect the increase of α-helix content during structural formation, since the proteins could be unfolded by lowering the temperature, which is referred to as

"cold denaturation" (Dias et al. 2010, Gulevsky and Relina 2013). With increasing NaCl concentrations, the negative molar ellipticity at 5°C decreased significantly, indicating the secondary structure formation of HjDHFR P1 as shown in Fig. III-3A, and a transition, which obeys the two-state unfolding model, was observed clearly as the temperature was increased. These results suggested that HjDHFR P1 has halophilic characteristics in its structural stability, and NaCl increased the structural stability of HjDHFR P1 mainly by inducing the formation of a stable structure.

The midpoint temperature of unfolding (T_m), the change in enthalpy with unfolding at T_m (ΔH_m), and the heat capacity change due to unfolding (ΔC_p) were calculated by nonlinear least-squares analysis using eqs. II-3 and II-4, and are listed in Table III-2. Accurate determination of these thermodynamic parameters indicated that the thermal unfolding of HjDHFR P1 essentially followed the two-state unfolding model, except for those at 0 and 100 mM NaCl. The T_m and ΔH_m values at 150 mM NaCl, 34.1 ± 0.0°C and 210.5 ± 2.1 kJ·mol^{-1}, respectively, increased to 58.2 ± 0.1°C and 283.5 ± 4.7 kJ·mol^{-1}, respectively, at 1,000 mM NaCl. Conversely, the ΔC_p value decreased 2-fold from 17.5 ± 0.4 kJ·mol^{-1}·K^{-1} at 150 mM NaCl to 8.5 ± 0.2 kJ·mol^{-1}·K^{-1} at 1,000 mM NaCl. The NaCl concentration dependence of these parameters was plotted in Fig. III-7B. As shown in these panels, T_m and ΔH_m clearly increased, but ΔC_p decreased as the NaCl concentration increased. It was noteworthy that the change of ΔC_p converged at 500 mM NaCl (Fig. III-7B), at which concentration structural formation also converged, as shown in Fig. III-4B, although other parameters changed moderately at more than 500 mM NaCl (Fig. III-7B).

III-2-5. Effects of salt on urea-induced unfolding

In addition, the effects of salt on the urea-induced unfolding of HjDHFR P1 were

measured by fluorescence spectra at 25°C and pH 8.0 under various NaCl concentrations. The CSM values were calculated using eq. II-1 and plotted against urea concentration in Fig. III-8A. Although the baseline of native state was unclear at 0 and 250 mM NaCl, the urea-induced unfolding of HjDHFR P1 essentially followed the two-state unfolding model. In addition, the transition clearly shifted to higher urea concentrations at increasing NaCl concentrations, again indicating the halophilic characteristics on the structural stability of HjDHFR P1.

The Gibbs free energy change in the absence of urea ($\Delta G°_u$), the urea concentration dependence of the free energy change (m), and the midpoint urea concentration of unfolding (C_m) at each NaCl concentration were calculated by nonlinear least-squares analysis using eqs. II-3 and II-5. The obtained parameters are listed in Table III-3. Since the baselines of the native and unfolded states were almost independent of NaCl concentration, I could determine the thermodynamic parameters at 0 and 250 mM NaCl assuming the same baselines as the higher NaCl concentrations. The obtained $\Delta G°_u$ and C_m values in the absence of NaCl were 2.0 ± 1.9 kJ·mol^{-1} and 0.6 ± 0.6 M, respectively. Previously, Ohmae et al. (2012) reported that the corresponding values for EcDHFR under the same conditions were 21.8 ± 1.8 kJ·mol^{-1} and 2.7 ± 0.3 M, respectively. Compared to EcDHFR, HjDHFR P1 was extremely unstable, and this finding agreed with the observation that it did not form a complete tertiary structure in the absence of NaCl. However, the $\Delta G°_u$ and C_m values of HjDHFR P1 in the presence of 750 mM NaCl, 21.5 ± 2.1 kJ·mol^{-1} and 2.7 ± 0.4 M, respectively, were coincident with those of EcDHFR in the absence of NaCl. Therefore, HjDHFR P1 has almost the same structural stability at 750 mM NaCl as EcDHFR in the absence of NaCl. Interestingly, the $\Delta G°_u$ and C_m values increased linearly against NaCl concentration, as shown in Fig. III-8B, and the

stabilization of HjDHFR P1 did not converge until 1,000 mM NaCl, suggesting that increasing NaCl concentrations stabilize HjDHFR P1 further, as reported previously for the stabilization of EcDHFR and two HvDHFRs by NaCl, KCl, and CsCl (Wright et al. 2002).

III-3. Effects of salt on the enzymatic function of HjDHFR P1

III-3-1. pH dependence of enzyme activity

To characterize the function of HjDHFR P1, the pH dependence of its enzymatic activity from pH 5.0 to 10.0 was measured in the absence or presence of 200 or 1,000 mM NaCl. As shown in Fig. III-9, the enzyme activity of HjDHFR P1 in the absence of NaCl was slightly pH dependent; the optimal pH was approximately 6.0, and its activity decreased moderately as the pH was increased above 6.0. When 200 mM NaCl was added to the reaction mixture, enzymatic activity was significantly enhanced in the neutral pH region (pH 5.0–8.0), although the optimal pH was not changed by the addition of NaCl. The ratio of enzymatic activity between pH 6.0 and 8.0 was 3.8 in the presence of 200 mM NaCl, but it was only 1.3 in the absence of NaCl.

The inset of Fig. III-9 shows on a logarithmic scale. The apparent pK_a and pK_b values obtained from fittings using eq. II-6 are listed in Table III-4. The activity of HjDHFR P1 without NaCl was obviously pH dependent; it was almost constant at the neutral pH region (5.2–8.0) and clearly decreased at the higher and lower pH regions with pK_a and pK_b values of 5.0 ± 0.2 and 8.4 ± 0.2, respectively. It is known that EcDHFR shows similar pH-dependent enzyme activity at neutral to basic pH region, and the rate-determining step of the enzymatic reaction is changed from the THF-releasing step at the neutral pH region to the hydride-transfer step at a pH greater than 8.4 (Fierke et al. 1987). Therefore, as for

EcDHFR, the rate-determining step of HjDHFR P1 above pH 8.4 was presumed to be the hydride-transfer step. However, the rate-determining step from the acidic to neutral pH region (pH 5.0–8.0) was unclear, because each of the two binding and two releasing steps could be a candidate, although the former could be eliminated if the DHF and NADPH concentrations in this experimental condition (both 50 μM) are excessive. The addition of NaCl clearly increased the enzymatic activity of HjDHFR P1 from the acidic to neutral pH region, but only had small effects above pH 8.5. Thus, NaCl accelerated the reaction rate of the rate-determining step at the acidic to neutral pH region, but did not enhance that at the basic pH region. The decrease of pK_b values from 8.4 to 7.4 by the addition of NaCl also indicated that the hydride-transfer step became the rate-determining step at pH 7.4–8.4 by accelerating the rate-determining step at this pH region. Conversely, decreased enzyme activity at pH 5 in the absence and presence of NaCl might suggest the contribution of another dissociable group to the enzymatic reaction of HjDHFR P1. However, aggregation of the enzyme could contribute because calculated pI of this enzyme is 4.8, and the reason for this observation was unclear because of poor data points at the acidic pH region.

III-3-2. Salt concentration dependence of enzyme activity

Fig. III-10 shows the NaCl concentration dependence of the enzyme activity of HjDHFR P1 at pH 6.0, 8.0, and 10.0. At pH 6.0, enzyme activity was enhanced approximately 8-fold by the addition of 500 mM NaCl, and conversely decreased by the further addition of NaCl. Even at 4,000 mM NaCl, HjDHFR P1 preserved about 105% of the activity observed in the absence of NaCl. At pH 8.0, only a 4-fold enhancement was observed at 250 mM NaCl, and the activity decreased gradually at higher concentrations

of NaCl. Finally, the enzyme activity of HjDHFR P1 became independent of NaCl concentration at pH 10.0. This result clearly indicated that the reaction rate of the rate-determining step at the neutral pH region depended on NaCl concentration, and that at pH 10 was independent of NaCl concentration. In addition, I measured the NaCl, TMACl, and CH_3COONa concentration dependences of the enzyme activity of HjDHFR P1 (inset of Fig. III-10). The difference in the activation effects between organic and inorganic cations and anions clearly indicated that chloride anions activated HjDHFR P1. These results clearly indicated that HjDHFR P1 has halophilic characteristics in its function compared to EcDHFR, which was inhibited by the addition of salt and lost about 50% activity at 250 mM NaCl (Ohmae et al. 2013a).

III-3-3. Deuterium isotope effects on steady-state kinetics

To clarify the relationship between the solvent environment (pH and NaCl concentration) and hydride-transfer rate in the catalytic cycle of HjDHFR P1, deuterium isotope effects on steady-state enzyme activity was measured. The isotope effects, ^{D}V, were evaluated by calculating the ratio of the initial velocities between using NADPH and NADPD as a cofactor, and are listed in Table III-5. David et al. (1992) reported that ^{D}V values in the steady-state turnover of EcDHFR could range from 1 to 3, and if the rate-determining step is hydride transfer, the ^{D}V value is close to 3. Conversely, if the rate-determining step is 3 times slower than the hydride-transfer rate, the ^{D}V value is close to 1. As shown in Table III-5, the ^{D}V values of HjDHFR P1 at pH 10.0 were 2.7–3.3, indicating that hydride transfer was fully rate-determining independent of NaCl concentration. This value was decreased to 1.0–1.2 at pH 6.0, indicating that hydride transfer was sufficiently faster than the rate-determining step at this pH. Conversely, the

^{D}V value at pH 8.0 increased from 1.5 to 2.8 as NaCl concentration increased from 0 to 1,000 mM, indicating that hydride transfer changed from partially rate-determining to fully rate-determining as the NaCl concentration increased. These data clearly showed that the activation mechanism of HjDHFR P1 by salt was unrelated to hydride transfer from NADPH to DHF.

III-3-4. Steady-state enzyme kinetics

To confirm that the DHF- and NADPH-binding steps could be eliminated as candidates for the rate-determining step at the neutral pH region, I determined the steady-state kinetics parameters of the enzymatic reaction of HjDHFR P1 at 25°C and pH 6.0 or 8.0 under several concentrations of NaCl. The obtained parameters are listed in Table III-6. At pH 6.0, the k_{cat} values for DHF and NADPH increased drastically from 3 to 20 s^{-1} as the NaCl concentration increased from 0 to 500 mM, similar to the activation profile of HjDHFR P1 at this pH (Fig. III-10). However, the K_m values for DHF and NADPH increased 4-fold and only slightly, respectively, by the addition of 500 mM NaCl. It is noteworthy that the maximum K_m values (8.1 ± 0.7 μM for both DHF and NADPH) were less than 10 μM. Thus, the DHF and NADPH concentrations used for the measurements of pH and salt concentration dependences (both 50 μM) could be considered to be in excess, and the binding steps of both substrates were not the rate-determining step at pH 6.0. Conversely, at pH 8.0, the k_{cat} values for DHF and NADPH increased only slightly from 1.5 to 3 s^{-1} as the NaCl concentration increased from 0 to 200 mM and decreased gradually at higher NaCl concentrations, which also matched the activation profile at this pH (Fig. III-10). In addition, the K_m values were almost independent of NaCl concentration considering experimental error, and the maximum values (8.5 ± 1.4 μM and

6.4 ± 1.1 μM for DHF and NADPH, respectively) were still less than 10 μM. Thus, the concentration of 50 μM could also be assumed to be in excess and the binding steps were also not the rate-determining step at pH 8.0.

III-3-5. Effects of NaCl concentration during pre-incubation

To check the maximum activation effect of chloride anions, I measured the enzyme activity of HjDHFR P1 at the pH 6.0 and 500 mM NaCl condition employing pre-incubation with various concentrations of NaCl. Fig. III-11A shows the time courses of the absorption changes initiated by the addition of the pre-incubated solution containing enzyme, NADPH, and various concentrations of NaCl to the DHF solution containing an appropriate concentration of NaCl to a final concentration of 500 mM. As shown in Fig. III-11A, the initial slope of the absorption change increased and the reaction ended faster as the NaCl concentration increased during pre-incubation. The reaction rates of the enzymatic reaction were calculated from the slopes of 60−90 s, and plotted against the NaCl concentration during pre-incubation (inset of Fig. III-11A). The reaction rate increased gradually as the NaCl concentration during pre-incubation increased from 0 to 1,000 mM, and became almost constant over 1,250 mM. It is noteworthy that the reaction rate increased continuously at more than 500 mM NaCl, in which the maximum activity is observed at this pH (Fig. III-10). This result clearly indicated that the activation effect of chloride anions continued over 500 mM, but higher concentrations of NaCl in the reaction mixture reduced the steady-state turnover rate of HjDHFR P1. To determine the dissociation constant, K_d, between the enzyme and chloride anion, the data were fitted to eq. II-8, which was derived from one-to-one binding of the enzyme and anion. The calculated K_d value was 1,430 ± 740 mM. Although this value seemed overestimation due

to activity measurements in the presence of 500 mM NaCl, its successful fitting indicated that binding of a chloride anion to HjDHFR P1 enhanced enzymatic activity.

When the reaction was initiated by the addition of the enzyme–DHF–salt mixture to the NADPH solution, similar results were also observed, and the calculated K_d value was 1,980 ± 850 mM (Fig. III-11B). However, it was noteworthy that when the enzyme–DHF solution without NaCl was mixed with the NADPH solution containing NaCl, the initial slope of the absorbance change at 0 s was very low. Then, the slope increased gradually as the reaction progressed up to 60 s and became constant. This observation indicated a slight acceleration of the enzyme reaction during the reaction period. Such an activation effect was not observed when the NaCl concentration during pre-incubation was more than 500 mM or the reaction was initiated by mixing the enzyme–NADPH and DHF solutions. Therefore, it seemed that DHF could not bind to HjDHFR P1 without NADPH or chloride anions. To confirm this point, I measured rapid-phase ligand-binding kinetics.

III-3-6. Rapid-phase ligand binding kinetics

To evaluate the effects of salt on the substrate-binding reactions of HjDHFR P1, the rapid-phase (shorter than 1 s) fluorescence quenching of intrinsic tryptophan side chains by the binding of DHF or NADPH was monitored at pH 6.0 and 24.5°C under various NaCl concentrations. Fig. III-12 shows typical results of the time courses of the fluorescence quenching by binding of DHF (Fig. III-12A) or NADPH (Fig. III-12B) to the enzyme. As shown in Fig. III-12A, the change in fluorescence due to binding of DHF was very small in the absence of NaCl, and it became large as NaCl concentration increased, although the concentrations of the enzyme and DHF were not changed. This result suggested that salt enhanced the binding of DHF to HjDHFR P1. The observed

fluorescence decay data were fitted to eq. II-9, and the obtained apparent rate constant, k_{app}, and amplitude, A, were plotted against NaCl concentration (Table III-7, inset of Fig. III-12A). The A value obviously increased as NaCl concentration increased, similar to the activation effect of chloride anions (inset of Fig. III-11A). However, k_{app} was almost independent of NaCl concentration in the range of 16 ± 7 s^{-1}. These results indicated that DHF could only bind to chloride anion-bound HjDHFR P1 molecules, but the binding rate of DHF was independent of NaCl concentration.

Conversely, fluorescence quenching by the binding of NADPH was very rapid in the absence of NaCl, and became slower as NaCl concentration increased (Fig. III-12B). The k_{app} value was decreased by 20-fold from 365 ± 68 s^{-1} to 16 ± 0 s^{-1} as NaCl concentration increased from 250 to 2,000 mM (inset of Fig. III-12B). The A value only increased by 4-fold from 0.19 ± 0.03 to 0.72 ± 0.03 as NaCl concentration increased from 250 to 1,000 mM, and slightly decreased under higher concentrations of NaCl. These results suggested that NADPH bound rapidly to chloride anion-unbound HjDHFR P1 molecules, and more slowly to the chloride anion-bound enzyme.

III-3-7. Association and dissociation rate constants of ligands

To obtain information for the effects of salt on the binding and releasing rates of ligands, the ligand concentration dependence of the k_{app} value was measured under various NaCl concentrations (Fig. III-13 and Tables III-9–III-11). As shown in Fig. III-13A, the k_{app} value increased as DHF concentration increased. Similar results were also obtained for NADPH (Fig. III-13B). However, fluorescence quenching by the binding of $NADP^+$ and THF was difficult to measure at pH 6.0; therefore, pH was raised to 8.0. As a result, THF binding became measurable (Fig. III-13C), but the binding of $NADP^+$ to

HjDHFR P1 could not be measured even at pH 8.0. From the slope and intercept of these plots, association and dissociation rate constants, k_{on} and k_{off}, respectively, were determined, plotted against NaCl concentration in the insets of Fig. III-13 and are listed in Table III-8. As shown in the insets of Fig. III-13A and C, the k_{on} values for DHF and THF seemed almost independent of NaCl concentration; however, the k_{off} values for THF decreased slightly as NaCl concentration increased, consistent with the decrease of the k_{cat} value at pH 8.0 (Table III-6). This result suggested that the THF-releasing step is the rate-determining step of HjDHFR P1 at the neutral pH region, similar to EcDHFR.

Conversely, those for NADPH were significantly, approximately 10-fold, decreased as NaCl concentration increased from 500 to 2,000 mM (inset of Fig. III-13B). Nevertheless, the k_{on} value of 0.42 ± 0.01 $\mu M^{-1}s^{-1}$ at 2,000 mM NaCl generated a binding rate of 21 s^{-1} for 50 μM NADPH. This rate is substantially faster than the rate-determining step at pH 6.0 and 2,000 mM NaCl (approximately 3 s^{-1}); therefore, the NADPH-binding step is not the rate-determining step of HjDHFR P1 at the neutral pH region. This speculation is also confirmed by the sufficiently small K_m value for NADPH (5.7 ± 0.5 μM), as mentioned above, although this value was measured at pH 8.0 and 1,000 mM NaCl (Table III-6).

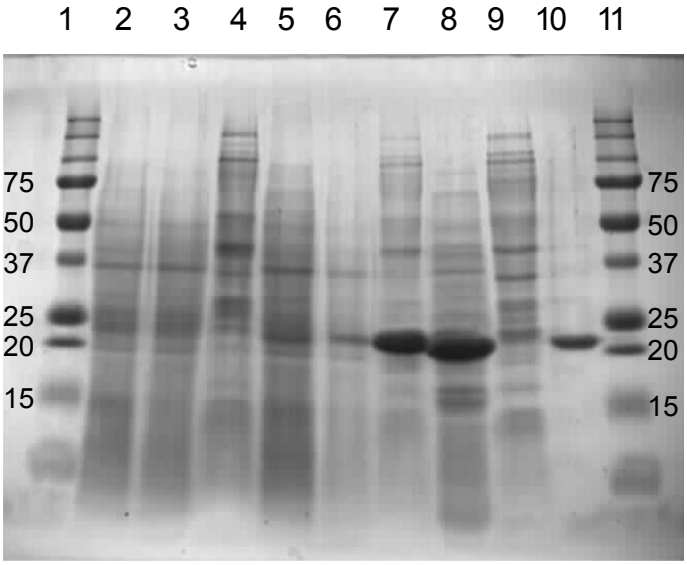

Fig. III-1. SDS-PAGE gel showing the overexpression of three DHFRs from *H. japonica* strain TR-1 in *E. coli*. Lanes 1 and 11: Molecular weight marker. Lanes 2, 3, and 4: Whole, soluble, and insoluble extracts of *E. coli* cells containing the HjDHFR C1 overexpression plasmid constructed from the pCold IV vector. Lanes 5, 6, and 7: The same as lanes 2, 3, and 4, respectively, except that *E. coli* contained the HjDHFR C2 overexpression plasmid constructed from the pET21a vector. Lanes 8 and 9: Soluble and insoluble extracts of *E. coli* containing the HjDHFR P1 overexpression plasmid constructed from the pUC118 vector. Lane 10: Purified HjDHFR P1 protein after refolding.

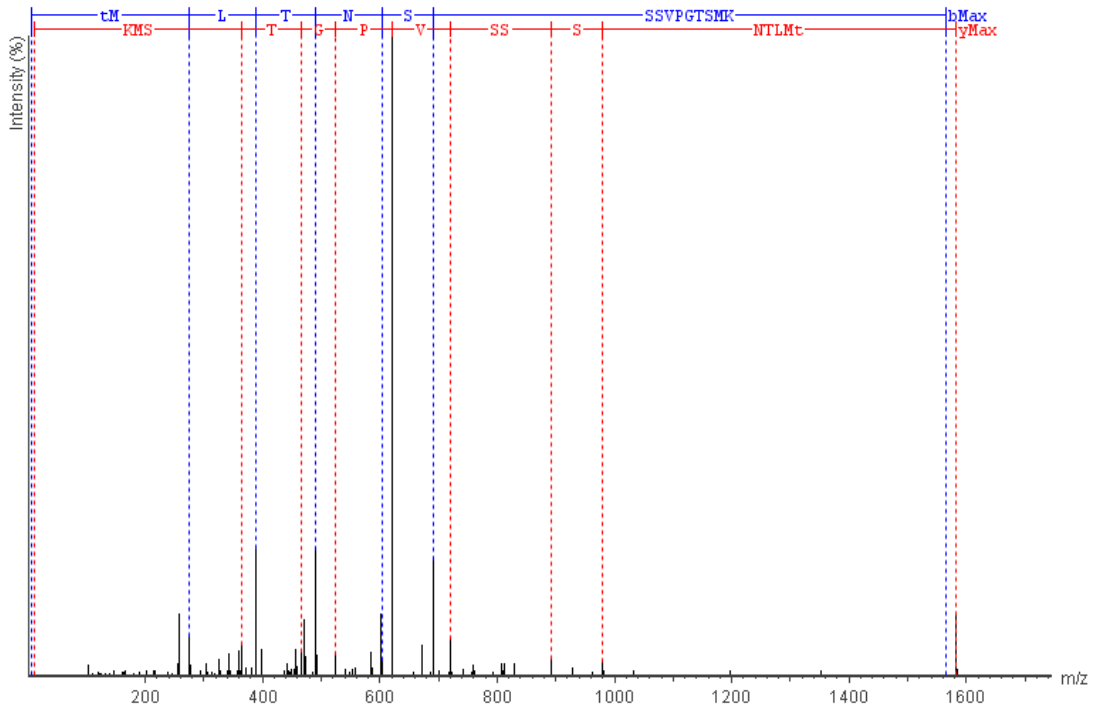

Fig. III-2. MS/MS analysis of the trypsin-digested N-terminus fragment of purified HjDHFR P1 protein. Amino acid sequence of the fragment (acetyl-TMITNSSSVPGTSMK) was determined by fragmentation patterns of b- and y- ions.

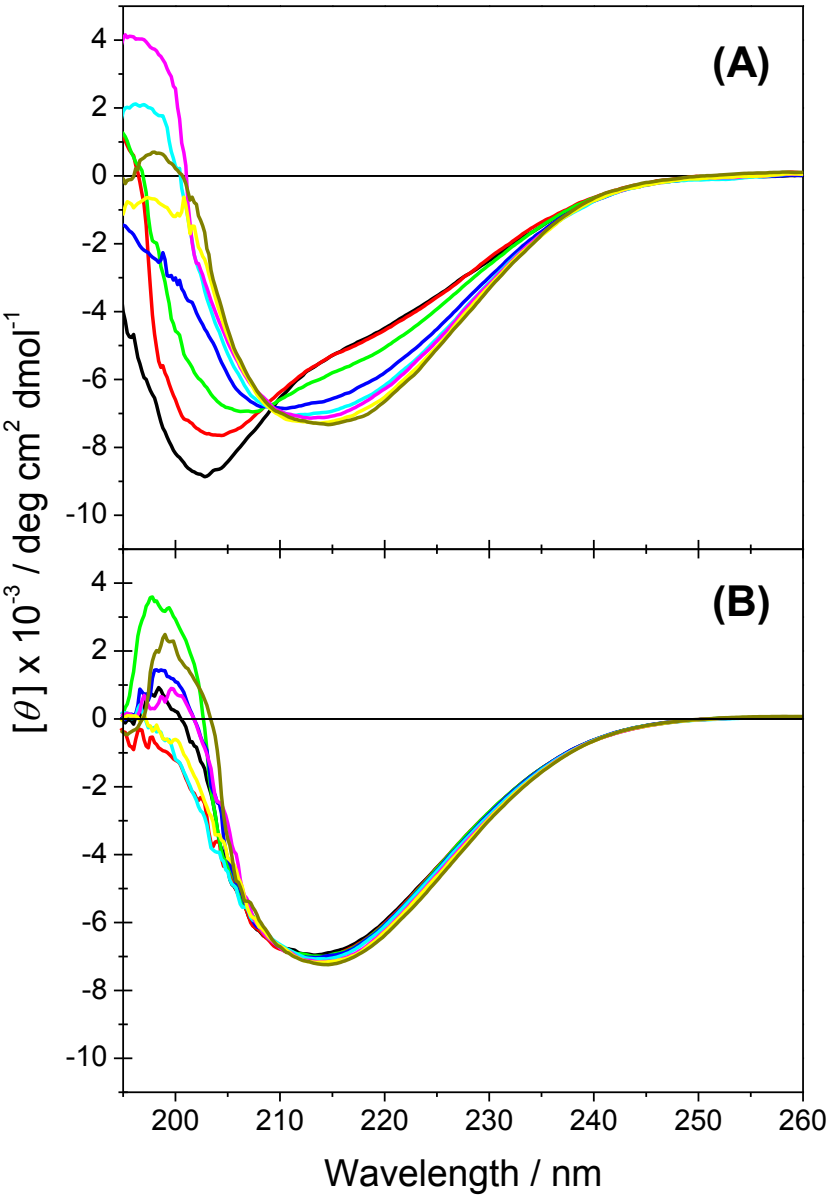

Fig. III-3. NaCl concentration dependence of the CD spectra of HjDHFR P1 at 25°C and pH 8.0 **(A)** or 6.0 **(B)**. NaCl concentrations are indicated by the following line colors: 0 (black), 50 (red), 100 (green), 200 (blue), 300 (cyan), 400 (magenta), 500 (yellow), and 1,000 mM (brown). The solvent used was TDE buffer (A) and 25 mM MES, 12.5 mM Tris, and 12.5 mM ethanolamine containing 0.05 mM dithiothreitol and 0.05 mM EDTA, whose pH was adjusted by acetic acid (B).

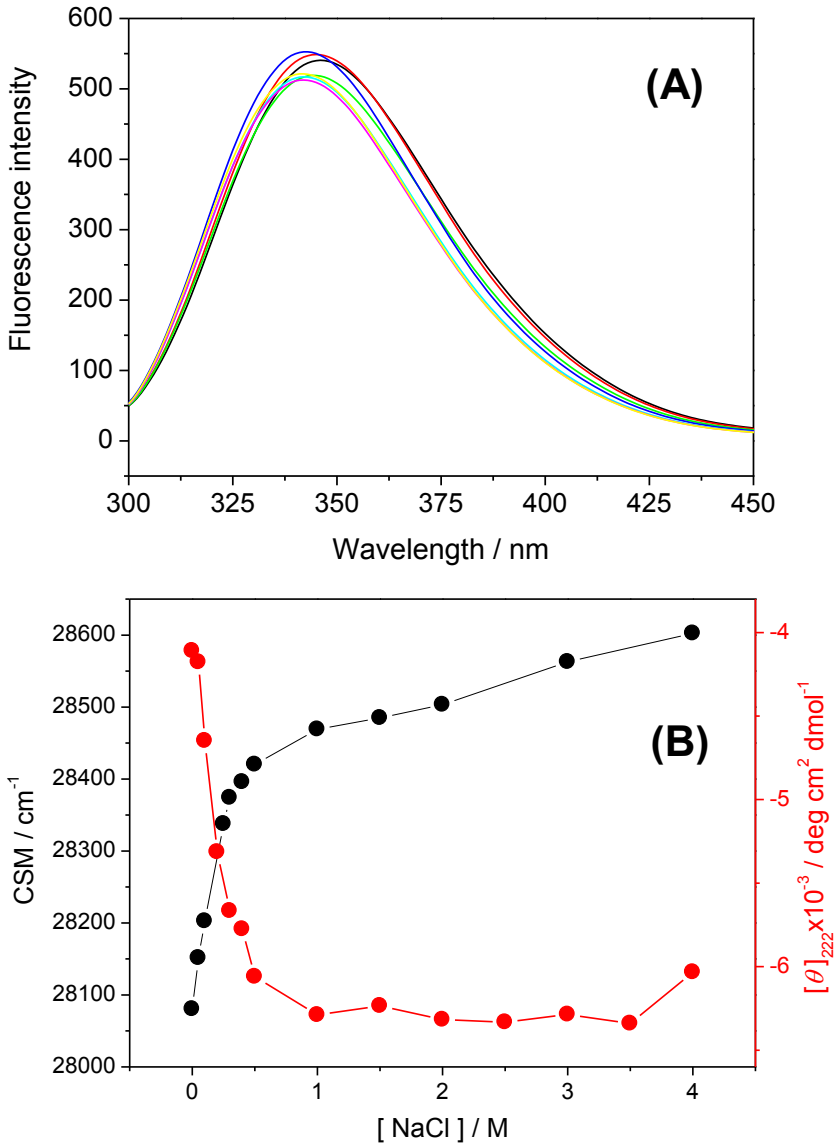

Fig. III-4. (A) NaCl concentration dependence of the fluorescence spectra of HjDHFR P1 at 25°C and pH 8.0. The solvent used was MTE buffer. NaCl concentrations are indicated by the following line colors: 0 (black), 50 (red), 100 (green), 200 (blue), 300 (cyan), 400 (magenta), 500 (yellow), and 1,000 mM (brown). **(B)** NaCl concentration dependence of the center of fluorescence spectral mass (CSM, black) and molar ellipticity at 222 nm ($[\theta]_{222}$, red) of HjDHFR P1 at 25°C and pH 8.0. The data values were calculated from Figs. III-4A and III-3A, respectively.

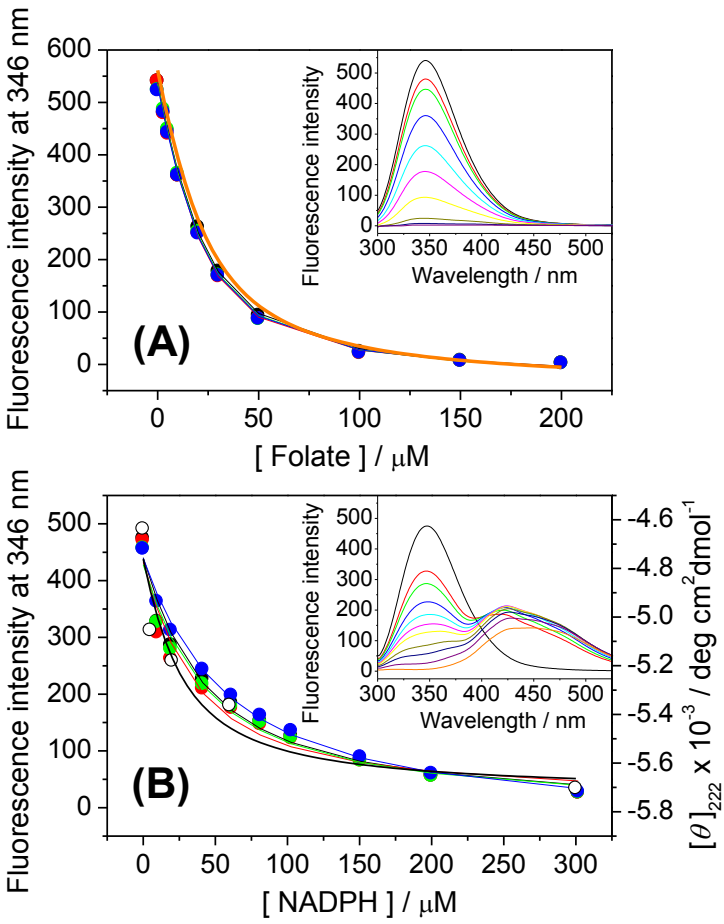

Fig. III-5. (A) Folate concentration dependence of the fluorescence intensity of HjDHFR P1 at 346 nm, 25°C, and pH 8.0. The solvent used was MTE buffer. NaCl concentration is indicated by the following colors: 0 (black), 200 (red), 500 (green), and 1,000 mM (blue). The solid lines indicate nonlinear least-squares fits to eq. II-2. Orange line indicates the folate concentration dependence of the L-tryptophan fluorescence in the absence of NaCl. **(B)** NADPH concentration dependence of the fluorescence intensity at 346 nm (closed circles) and molar ellipticity at 222 nm (open circles) of HjDHFR P1 at 25°C, and pH 8.0. The solvent used was MTE and TDE buffers for the fluorescence and CD measurements, respectively. Colors and lines are the same as panel (A). **Insets** show folate **(A)** and NADPH **(B)** concentration dependence of the fluorescence spectra of HjDHFR P1 in the absence of NaCl. (A) Folate concentrations are indicated by the following line colors: 0 (black), 3 (red), 5 (green), 10 (blue), 20 (cyan), 30 (magenta), 50 (yellow), 100 (brown), 150 (navy), and 200 μM (purple). (B) NADPH concentrations are indicated by the following line colors: 0 (black), 10 (red), 20 (green), 40 (blue), 60 (cyan), 80 (magenta), 100 (yellow), 150 (brown), 200 (navy), 300 (purple), and 500 μM (orange).

Table III-1. Dissociation constants between HjDHFR P1 and NADPH at 25°C, pH 8.0 and various concentrations of NaCl[a].

NaCl / mM	K_d / μM	
	fluorescence	CD
0	33.7 ± 9.6	19.5 ± 20.7
200	26.1 ± 9.4	NM
500	33.8 ± 8.6	NM
1,000	47.1 ± 6.1	NM

[a]The solvent used was MTE buffer. NM, not measured.

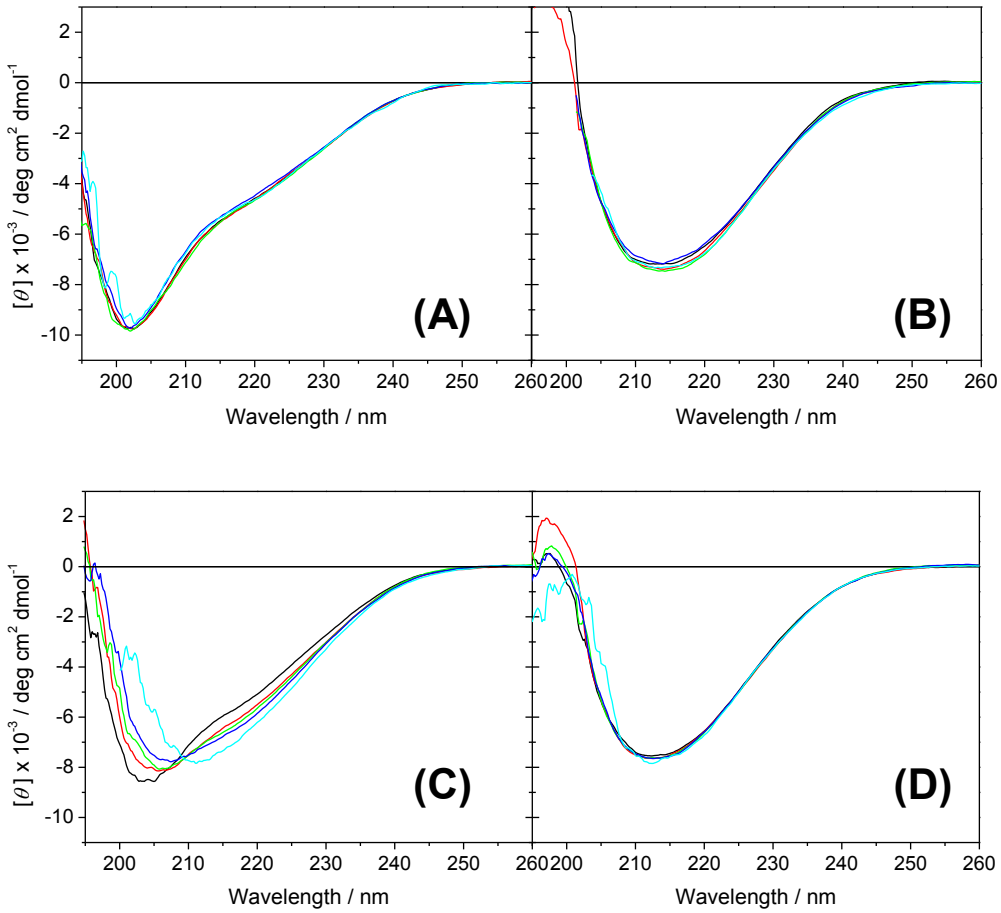

Fig. III-6. Folate **(A** and **B)** and NADPH **(C** and **D)** concentration dependence of the CD spectra of HjDHFR P1 at 25°C and pH 8.0. NaCl concentrations are 0 (panels A and C) and 500 mM (panels B and D). The solvent used was TDE buffer. The ligand concentrations are indicated by the following line colors: 0 (black), 5 (red), 20 (green), 60 (blue), and 300 µM (cyan).

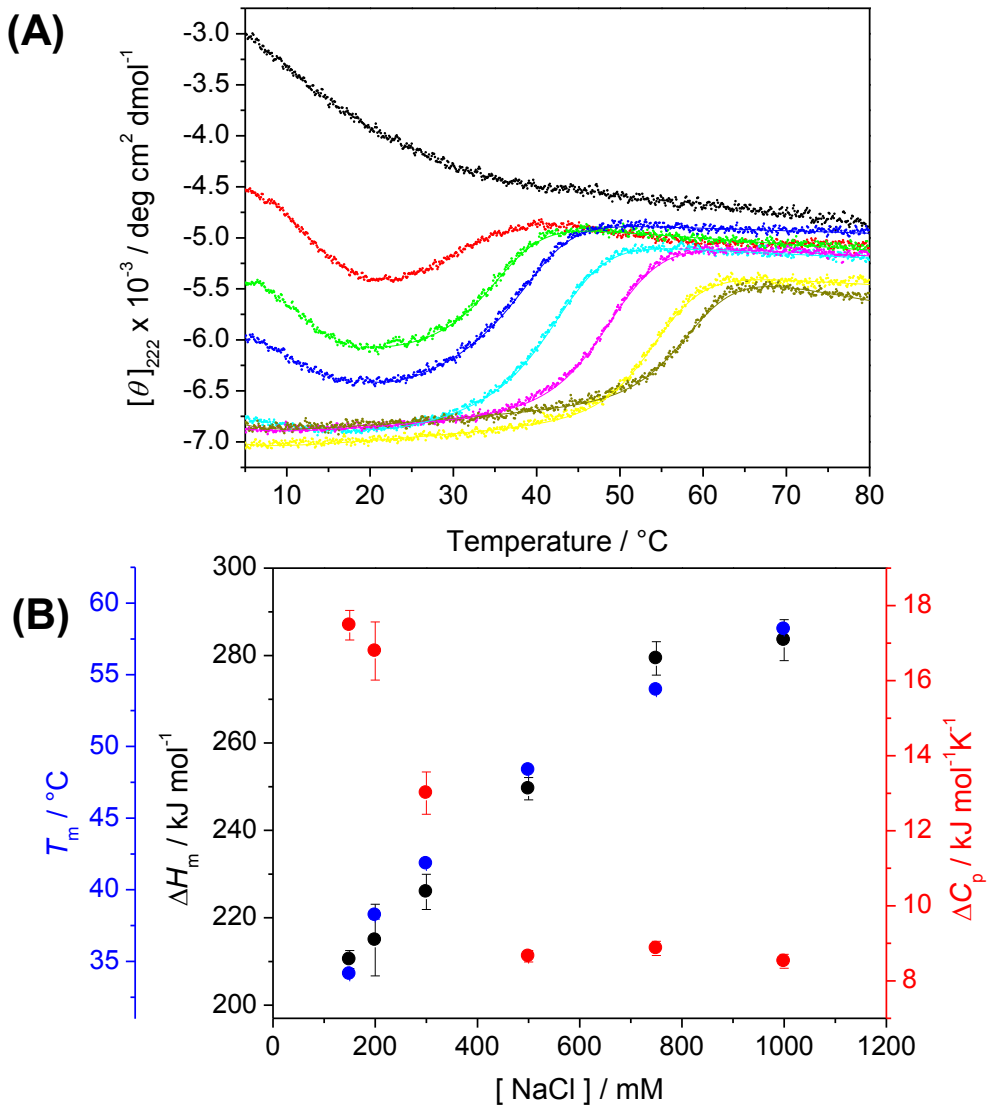

Fig. III-7. (A) Temperature dependence of molar ellipticity at 222 nm of HjDHFR P1 at pH 8.0 and various concentrations of NaCl. The solvent used was TDE buffer. NaCl concentrations are indicated by the following colors: 0 (black), 100 (red), 150 (green), 200 (blue), 300 (cyan), 500 (magenta), 750 (yellow), and 1,000 mM (brown). The solid lines indicate nonlinear least-squares fits to the two-state unfolding model (eqs. II-3 and II-4). Panel **(B)** shows the NaCl concentration dependence of the obtained thermodynamic parameters, T_m (blue), ΔH_m (black), and ΔC_p (red).

Table III-2. Thermodynamic parameters due to the thermal unfolding of HjDHFR P1 at pH 8.0 and various concentrations of NaCl[a].

NaCl / mM	T_m / °C	ΔH_m / kJ·mol^{-1}	ΔC_p / kJ·mol^{-1}·K^{-1}
0	ND	ND	ND
100	ND	ND	ND
150	34.1 ± 0.0	210.5 ± 2.1	17.5 ± 0.4
200	38.2 ± 0.3	214.9 ± 8.2	16.8 ± 0.8
300	41.8 ± 0.1	225.9 ± 4.0	13.0 ± 0.6
500	48.4 ± 0.0	249.5 ± 2.5	8.7 ± 0.2
750	54.0 ± 0.1	279.3 ± 3.8	8.9 ± 0.2
1,000	58.2 ± 0.1	283.5 ± 4.7	8.5 ± 0.2

[a]The solvent used was TDE buffer. ND, Not determined.

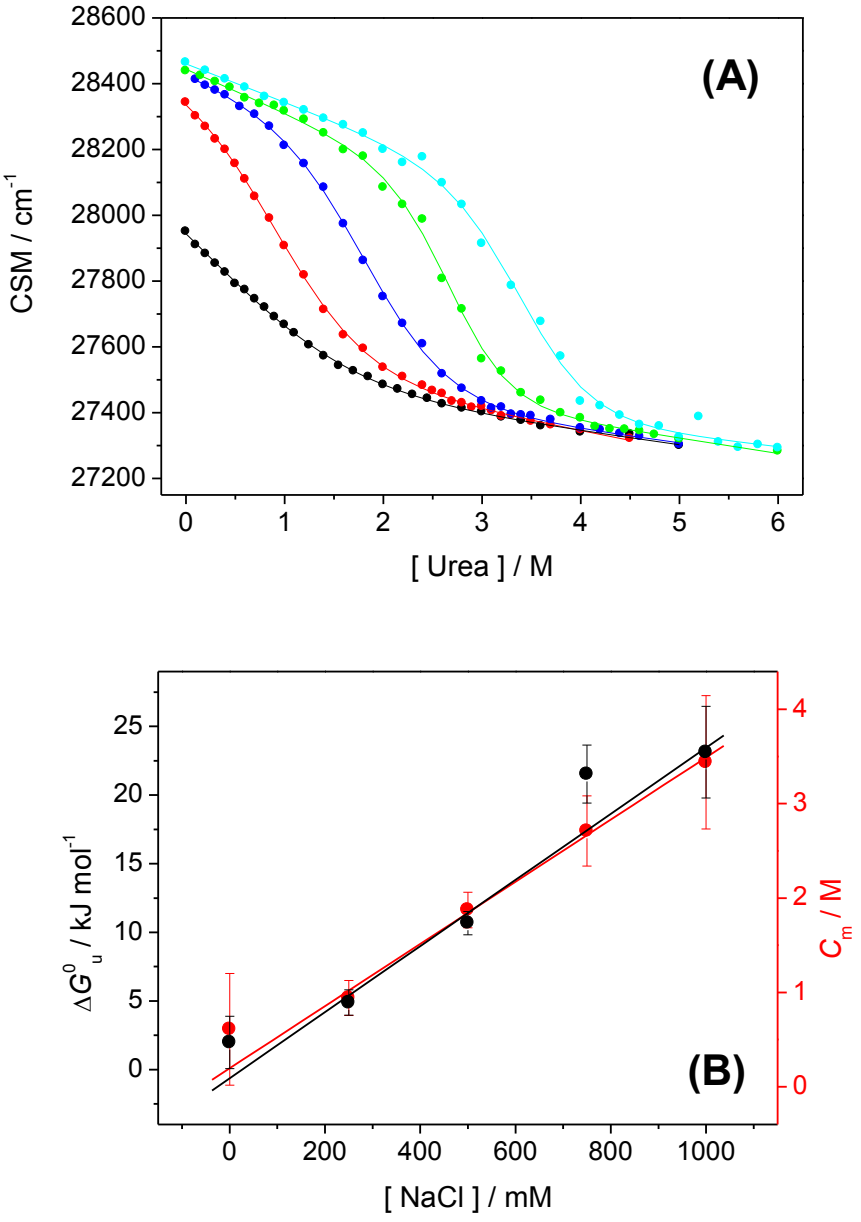

Fig. III-8. (A) Urea concentration dependence of the center of fluorescence spectral mass (CSM) of HjDHFR P1 at 25°C, pH 8.0, and various concentrations of NaCl. The solvent used was TDE buffer. NaCl concentrations are indicated by the following colors: 0 (black), 250 (red), 500 (blue), 750 (green), and 1,000 mM (cyan). The solid lines indicate nonlinear least-squares fits to the two-state unfolding model (eqs. II-3 and II-5). Panel **(B)** shows the NaCl concentration dependence of the obtained thermodynamic parameters, $\Delta G°_u$ (black) and C_m (red). The solid lines indicate least-squares linear fits.

Table III-3. Thermodynamic parameters due to the urea-induced unfolding of HjDHFR P1 at 25°C, pH 8.0, and various concentrations of NaCl[a].

DHFR	NaCl / mM	$\Delta G°_u$ / kJ·mol^{-1}	m / kJ·mol^{-1}·M^{-1}	C_m / M
HjDHFR P1	0	2.0 ± 1.9	3.3 ± 0.5	0.6 ± 0.6
	250	4.9 ± 0.9	5.2 ± 0.3	0.9 ± 0.2
	500	10.7 ± 0.8	5.7 ± 0.3	1.9 ± 0.2
	750	21.5 ± 2.1	7.9 ± 0.8	2.7 ± 0.4
	1,000	23.1 ± 3.3	6.7 ± 1.0	3.4 ± 0.7
EcDHFR[b]	0	21.8 ± 1.8	8.2 ± 0.7	2.7 ± 0.3

[a]The solvent used was TDE buffer. [b]Taken from Ohmae et al. (2012).

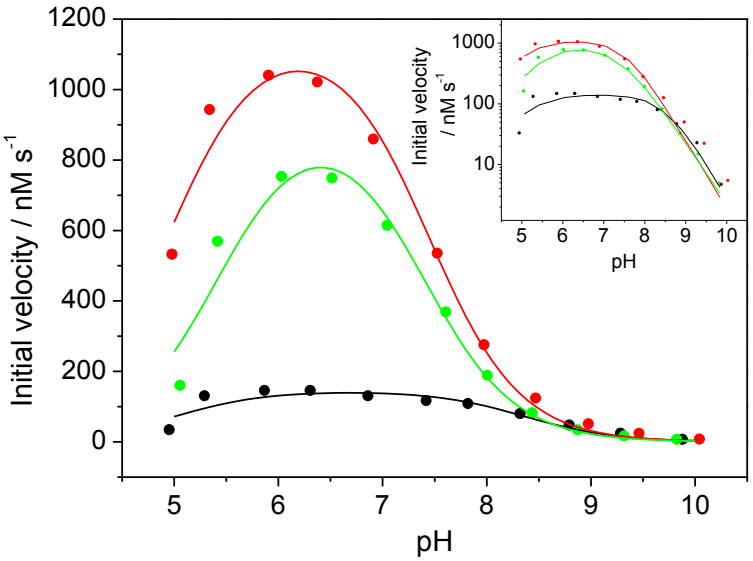

Fig. III-9. pH dependence of the enzymatic activity of HjDHFR P1 at 25°C under 0 (black), 200 (red), and 1,000 mM (green) NaCl. The buffer used was MTE buffer. The lines indicate nonlinear least-squares fits to eq. II-6. **Inset** shows on a logarithmic scale.

Table III-4. pK_a and pK_b values calculated from the pH dependence of the enzyme activity of HjDHFR P1.[a]

NaCl / mM	pK_a	pK_b
0	5.0 ± 0.2	8.4 ± 0.2
200	4.9 ± 0.1	7.4 ± 0.1
1,000	5.4 ± 0.1	7.4 ± 0.1

[a]The buffer used was MTE buffer.

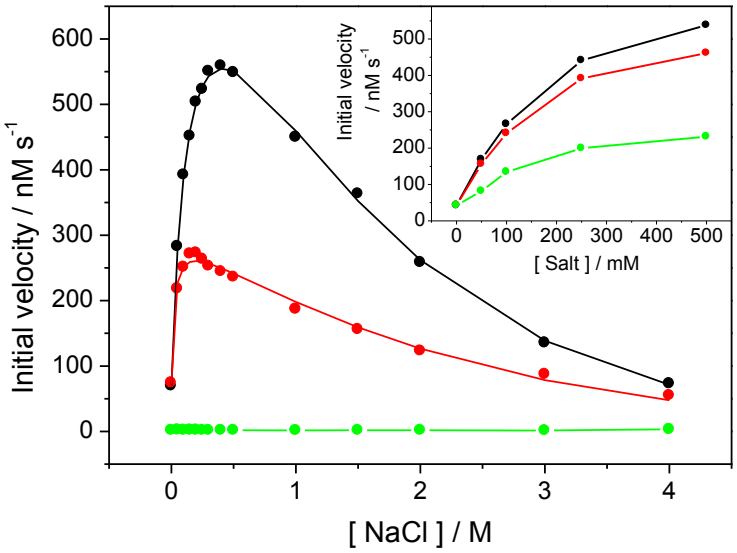

Fig. III-10. NaCl concentration dependence of the enzymatic activity of HjDHFR P1 at 25°C and pH 6.0 (black), 8.0 (red), and 10.0 (green). The lines indicate nonlinear least-squares fits to eq. IV-13 (see section IV-3-1). **Inset**: NaCl (black), TMACl (red), and CH_3COONa (green) concentration dependences of the enzymatic activity of HjDHFR P1 at 25°C and pH 8.0. The buffer used was MTE buffer.

Table III-5. Deuterium isotope effects (^{D}V) on the initial velocity of the steady-state enzymatic reaction of HjDHFR P1 at 25°C and various pH and NaCl concentrations.[a]

NaCl / mM	pH		
	6.0	8.0	10.0
0	1.0 ± 0.1	1.5 ± 0.0	2.7 ± 0.1
100	1.1 ± 0.0	2.2 ± 0.0	3.3 ± 0.6
200	1.2 ± 0.0	2.5 ± 0.0	3.3 ± 0.1
1,000	1.1 ± 0.0	2.8 ± 0.0	2.8 ± 0.1

[a]The buffer used was MTE buffer.

Table III-6. Steady-state kinetic parameters for the enzymatic reaction of HjDHFR P1 at 25°C.[a]

pH	NaCl / mM	DHF			NADPH		
		K_m / μM	k_{cat} / s^{-1}	(k_{cat}/K_m) / μM^{-1} s^{-1}	K_m / μM	k_{cat} / s^{-1}	(k_{cat}/K_m) / μM^{-1} s^{-1}
6.0	0	2.1 ± 0.6	3.4 ± 0.4	1.6 ± 0.5	6.6 ± 1.5	2.5 ± 0.1	0.4 ± 0.1
	200	5.1 ± 0.8	11.7 ± 0.5	2.3 ± 0.4	2.7 ± 0.1	8.5 ± 0.1	3.2 ± 0.2
	500	8.1 ± 0.7	20.7 ± 0.5	2.5 ± 0.2	8.1 ± 0.7	20.3 ± 0.5	2.5 ± 0.2
8.0	0	8.5 ± 1.4	1.5 ± 0.1	0.2 ± 0.0	6.4 ± 1.1	1.4 ± 0.1	0.2 ± 0.0
	200	8.9 ± 1.6	3.1 ± 0.2	0.4 ± 0.1	5.3 ± 1.4	3.2 ± 0.2	0.6 ± 0.2
	500	8.0 ± 0.7	2.7 ± 0.1	0.3 ± 0.0	3.6 ± 0.8	2.8 ± 0.1	0.8 ± 0.2
	1,000	NM	NM	NM	5.7 ± 0.5	2.0 ± 0.0	0.4 ± 0.2

[a]The buffer used was MTE buffer. NM, not measured.

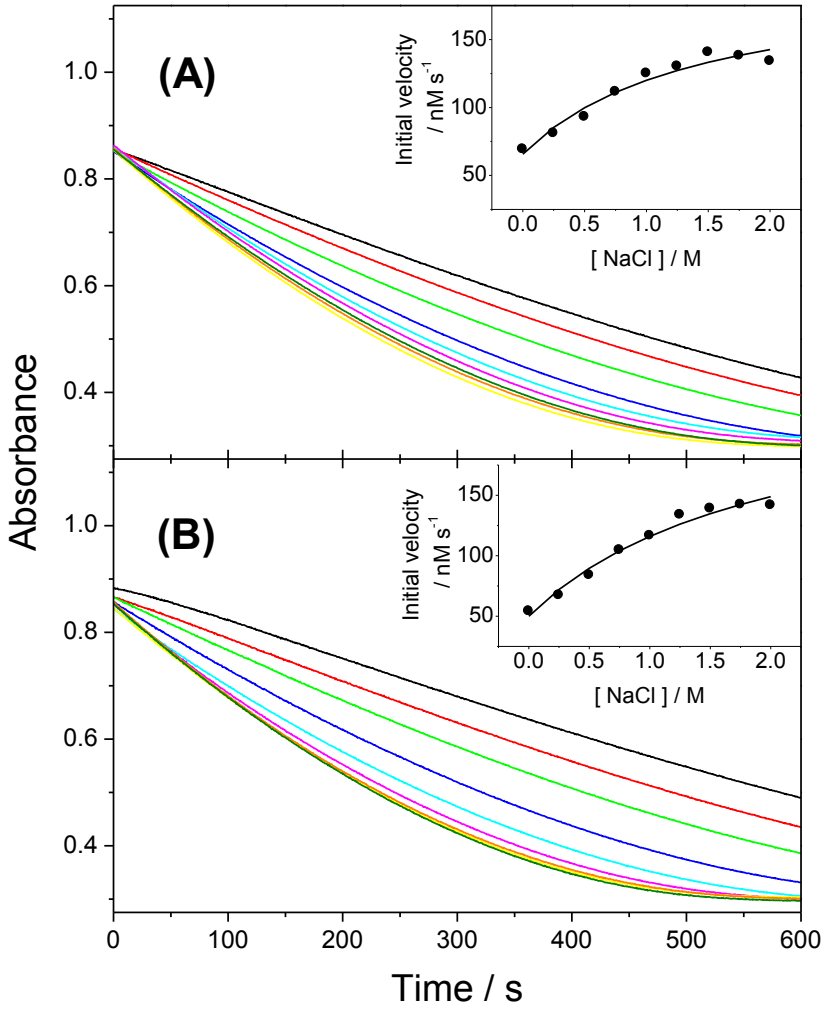

Fig. III-11. Time course of the absorption at 340 nm due to the enzymatic reaction of HjDHFR P1 at 25°C and pH 6.0 as a function of NaCl concentration during pre-incubation. The enzymatic reaction was initiated by the addition of an enzyme–DHF–NaCl mixture to an NADPH solution containing NaCl to a final concentration of 500 mM **(A)** or an enzyme–NADPH–NaCl mixture to a DHF solution containing NaCl to a final concentration of 500 mM **(B)**. The buffer used was MTE buffer. NaCl concentrations during pre-incubation are indicated by the following colors: 0 (black), 250 (red), 500 (green), 750 (blue), 1,000 (cyan), 1,250 (magenta), 1,500 (yellow), 1,750 (orange), and 2,000 mM (dark green). **Insets**: Plots of initial velocities as a function of NaCl concentration during pre-incubation. The solid lines indicate nonlinear least-squares fits to the simple one-to-one binding model (eq. II-8).

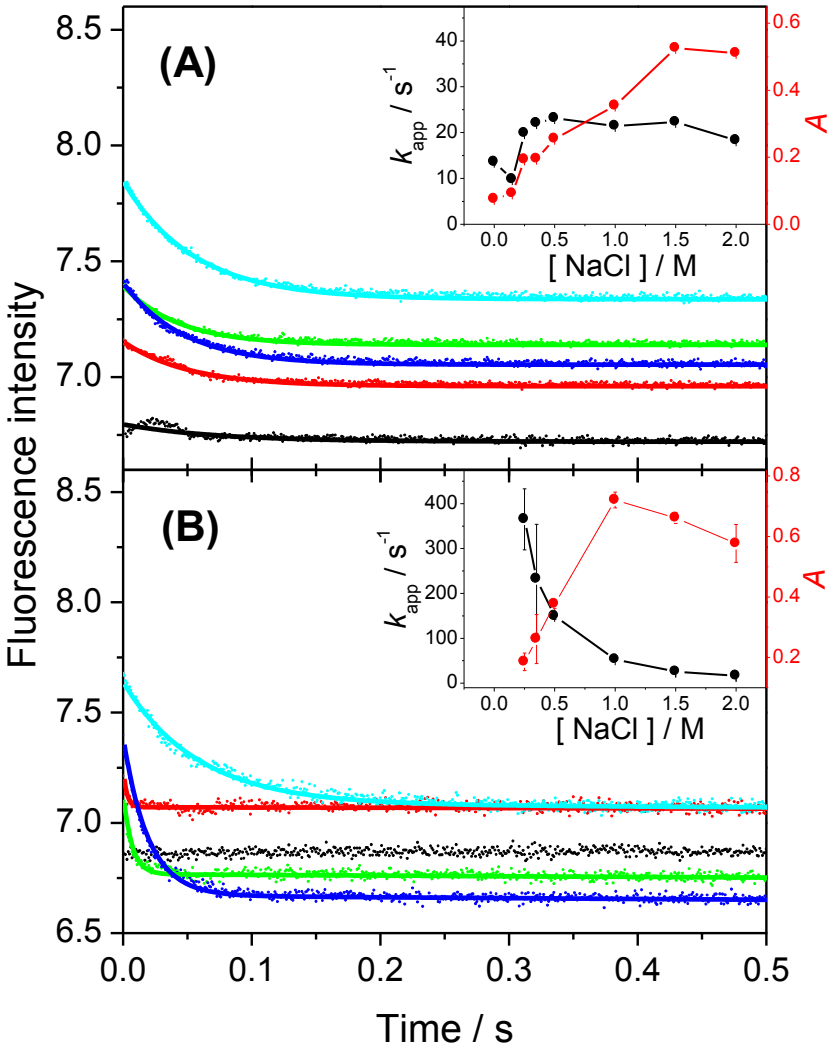

Fig. III-12. Quenching of intrinsic tryptophan fluorescence by rapid binding of DHF **(A)** or NADPH **(B)** to HjDHFR P1 at 24.5°C and pH 6.0 under various NaCl concentrations. The buffer used was MTE buffer and the concentrations of enzyme, DHF, and NADPH were 4.8, 50, and 25 μM, respectively. NaCl concentrations are indicated by the following colors: 0 (black), 250 (red), 500 (green), 1,000 (blue), and 2,000 mM (cyan). The solid lines indicate nonlinear least-squares fits to the single exponential with linear decay (eq. II-9). **Insets**: NaCl concentration dependence of the apparent rate constant (black) and amplitude parameter (red) of the exponential phase.

Table III-7. Obtained fitting parameters for the rapid-phase ligand binding reaction of HjDHFR P1 at pH 6.0 and 24.5°C.[a]

NaCl / mM	DHF				NADPH			
	A	k_{app} / s^{-1}	k_{lin} / s^{-1}	F_∞	A	k_{app} / s^{-1}	k_{lin} / s^{-1}	F_∞
0	0.07 ± 0.00	13.6 ± 0.7	0[b]	6.72 ± 0.00	ND	ND	ND	ND
150	0.09 ± 0.00	9.8 ± 0.4	0[b]	6.83 ± 0.00	ND	ND	ND	ND
250	0.19 ± 0.00	19.8 ± 0.3	0[b]	6.96 ± 0.00	0.19 ± 0.03	365.0 ± 68.0	–0.01 ± 0.00	7.07 ± 0.00
350	0.20 ± 0.00	22.0 ± 0.4	0[b]	7.10 ± 0.00	0.26 ± 0.08	232.4 ± 121.4	–0.04 ± 0.01	7.02 ± 0.01
500	0.26 ± 0.00	23.1 ± 0.3	0[b]	7.14 ± 0.00	0.38 ± 0.01	149.7 ± 7.3	–0.03 ± 0.00	6.77 ± 0.00
1,000	0.35 ± 0.00	21.4 ± 0.3	0[b]	7.05 ± 0.00	0.72 ± 0.03	53.0 ± 3.9	–0.04 ± 0.00	6.65 ± 0.04
1,500	0.53 ± 0.00	22.3 ± 0.2	0[b]	6.93 ± 0.00	0.66 ± 0.02	25.9 ± 0.0	–0.04 ± 0.00	6.59 ± 0.03
2,000	0.51 ± 0.00	18.3 ± 0.1	0[b]	7.34 ± 0.00	0.58 ± 0.06	16.4 ±0.0	–0.03 ± 0.00	7.13 ± 0.03

[a]The buffer used was MTE buffer. [b]The value was fixed to zero during fitting since it was negligibly small. ND, not detected.

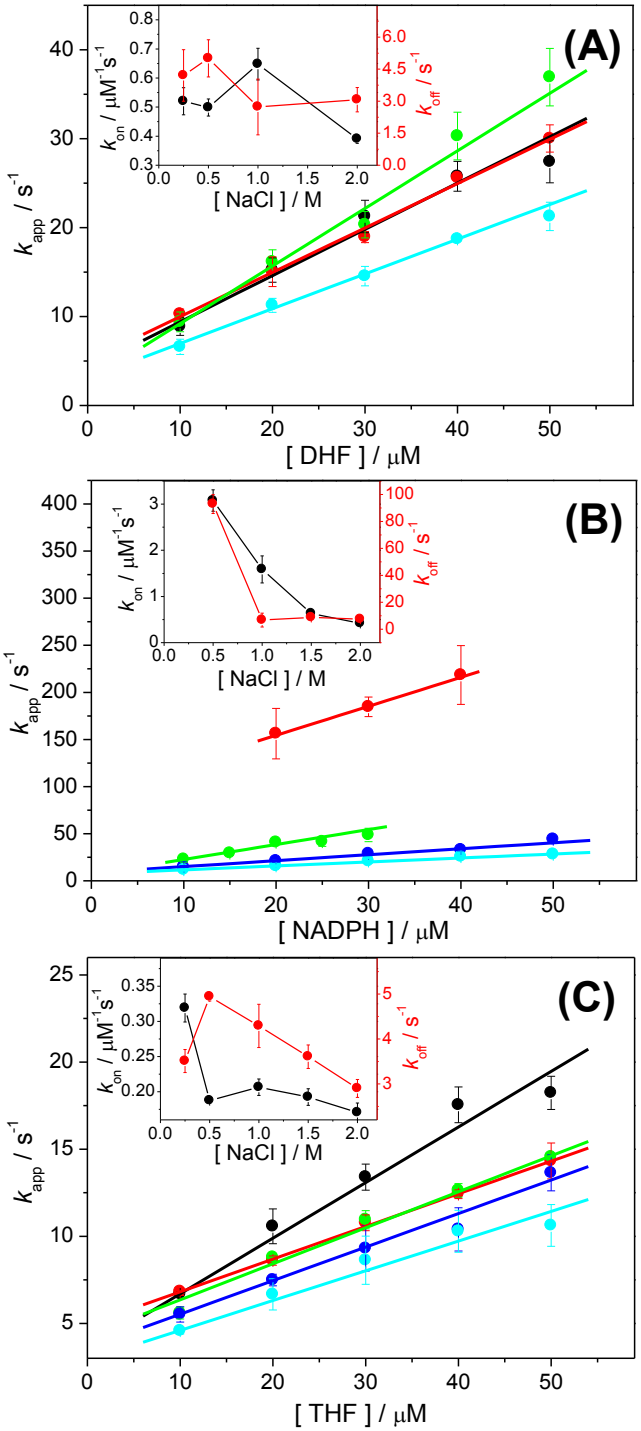

Fig. III-13. NaCl concentration dependence of association (black) and dissociation (red) rate constants for DHF **(A)**, NADPH **(B)**, and THF **(C)** to HjDHFR P1 at 24.5°C. The buffer used was MTE buffer whose pH was adjusted to 6.0 (A and B) or 8.0 (C) by acetic acid or TMAOH, respectively. **Insets**: Ligand concentration dependence of the apparent rate constants for the binding at various NaCl concentrations. NaCl concentrations are indicated by the following colors: 250 (black), 500 (red), 1,000 (green), 1,500 (blue), and 2,000 mM (cyan). The lines indicate least squares linear fits.

Table III-8. Association and dissociation rate constants between ligands and HjDHFR P1 at pH 6.0 and 24.5°C.[a]

NaCl / mM	DHF		NADPH		THF[b]	
	k_{on} / μM^{-1} s^{-1}	k_{off} / s^{-1}	k_{on} / μM^{-1} s^{-1}	k_{off} / s^{-1}	k_{on} / μM^{-1} s^{-1}	k_{off} / s^{-1}
250	0.52 ± 0.05	4.2 ± 1.2	ND	ND	0.32 ± 0.02	3.5 ± 0.3
500	0.50 ± 0.03	5.0 ± 0.9	3.1 ± 0.2	92.9 ± 6.7	0.19 ± 0.00	4.9 ± 0.1
1,000	0.65 ± 0.05	2.7 ± 1.3	1.6 ± 0.3	6.8 ± 5.1	0.21 ± 0.01	4.3 ± 0.5
1,500	NM	NM	0.63 ± 0.05	8.8 ± 1.4	0.19 ± 0.01	3.6 ± 0.3
2,000	0.39 ± 0.02	3.1 ± 0.6	0.42 ±0.01	7.5 ± 0.3	0.17 ± 0.01	2.9 ± 0.2

[a]The buffer used was MTE buffer. [b]The values for THF were measured at pH 8.0. ND, not detected; NM, not measured.

Table III-9. Obtained fitting parameters for the rapid-phase DHF-binding reaction of HjDHFR P1 at pH 6.0 and 24.5°C.[a]

NaCl / mM	DHF / μM	A	k_{app} / s^{-1}	k_{lin} / s^{-1}	F_∞
250	10	0.23 ± 0.03	8.9 ± 1.0	0[b]	8.52 ± 0.03
	20	0.32 ± 0.04	15.2 ± 1.4	0	8.30 ± 0.05
	30	0.34 ± 0.07	21.3 ± 1.8	0	8.03 ± 0.02
	40	0.32 ± 0.05	25.8 ± 1.7	0	7.91 ± 0.05
	50	0.24 ± 0.04	27.4 ± 2.4	0	7.72 ± 0.03
500	10	0.42 ± 0.01	10.3 ± 0.6	0	8.36 ± 0.01
	20	0.50 ± 0.08	15.0 ± 1.7	0	8.09 ± 0.03
	30	0.44 ± 0.04	18.9 ± 0.6	0	7.93 ± 0.02
	40	0.50 ± 0.07	25.6 ± 0.6	0	7.68 ± 0.02
	50	0.47 ± 0.09	30.0 ± 1.5	0	7.49 ± 0.01
1,000	10	0.25 ± 0.03	9.4 ± 1.1	0	7.61 ± 0.02
	20	0.29 ± 0.01	16.2 ± 1.3	0	8.77 ± 0.02
	30	0.26 ± 0.01	20.3 ± 1.5	0	8.23 ± 0.01
	40	0.23 ± 0.02	30.3 ± 2.7	0	8.78 ± 0.00
	50	0.23 ± 0.01	36.9 ± 3.2	0	9.30 ± 0.02
2,000	10	0.19 ± 0.01	6.6 ± 0.9	0	6.49 ± 0.02
	20	0.26 ± 0.03	11.3 ± 0.8	0	7.14 ± 0.01
	30	0.28 ± 0.02	14.5 ± 1.1	0	8.05 ± 0.01
	40	0.25 ± 0.02	18.7 ± 0.2	0	9.12 ± 0.02
	50	0.23 ± 0.01	21.3 ± 1.6	0	9.72 ± 0.01

[a]The buffer used was MTE buffer. [b]The value was fixed to zero during fitting since it was negligibly small.

Table III-10. Obtained fitting parameters for the rapid-phase NADPH-binding reaction of HjDHFR P1 at pH 6.0 and 24.5°C.[a]

NaCl / mM	NADPH / μM	A	k_{app} / s^{-1}	k_{lin} / s^{-1}	F_∞
500	20	0.29 ± 0.04	156.3 ± 26.8	–0.27 ± 1.27	7.79 ± 0.10
	30	0.26 ± 0.06	184.7 ± 10.4	–0.49 ± 0.02	7.40 ± 0.00
	40	0.29 ± 0.02	218.4 ± 31.2	0.38 ± 0.38	7.04 ± 0.03
1,000	10	0.43 ± 0.05	22.7 ± 2.9	–0.04 ± 0.01	8.83 ± 0.08
	15	0.55 ± 0.05	29.3 ± 1.7	–0.02 ± 0.02	8.71 ± 0.04
	20	0.58 ± 0.00	41.0 ± 1.8	–0.03 ± 0.0	8.55 ± 0.05
	25	0.64 ± 0.02	41.5 ± 4.9	–0.03 ± 0.00	8.35 ± 0.02
	30	0.71 ± 0.00	48.6 ± 7.1	–0.03 ± 0.00	8.15 ± 0.02
1,500	10	0.48 ± 0.00	15.1 ± 1.0	–0.03 ± 0.01	9.07 ± 0.02
	20	0.46 ± 0.05	21.0 ± 1.3	–0.02 ± 0.01	8.76 ± 0.07
	30	0.58 ± 0.10	28.9 ± 1.2	–0.04 ± 0.00	8.49 ± 0.03
	40	0.72 ± 0.01	32.9 ± 1.0	–0.02 ± 0.01	8.12 ± 0.02
	50	0.68 ± 0.07	44.1 ± 2.9	–0.03 ± 0.01	7.86 ± 0.05
2,000	10	0.42 ± 0.02	11.6 ± 0.3	–0.04 ± 0.00	9.50 ± 0.04
	20	0.45 ± 0.05	15.8 ± 0.8	–0.03 ± 0.01	9.11 ± 0.07
	30	0.56 ± 0.10	20.9 ± 2.3	–0.02 ± 0.01	8.74 ± 0.06
	40	0.56 ± 0.12	25.6 ± 1.3	–0.03 ± 0.01	8.42 ± 0.02
	50	0.52 ± 0.07	28.1 ± 0.7	–0.02 ± 0.00	8.17 ± 0.04

[a]The buffer used was MTE buffer.

Table III-11. Obtained fitting parameters for the rapid-phase THF-binding reaction of HjDHFR P1 at pH 8.0 and 24.5°C.[a]

NaCl / mM	THF / μM	A	k_{app} / s^{-1}	k_{lin} / s^{-1}	F_∞
250	10	0.03 ± 0.00	6.7 ± 0.1	0[b]	2.48 ± 0.00
	20	0.06 ± 0.00	10.6 ± 1.0	0	3.47 ± 0.00
	30	0.08 ± 0.00	13.4 ± 0.7	0	4.38 ± 0.00
	40	0.09 ± 0.00	17.5 ± 1.0	0	5.39 ± 0.00
	50	0.12 ± 0.00	18.2 ± 1.0	0	6.38 ± 0.00
500	10	0.05 ± 0.00	6.8 ± 0.2	0	2.71 ± 0.00
	20	0.06 ± 0.01	8.6 ± 0.3	0	3.89 ± 0.00
	30	0.08 ± 0.01	10.8 ± 0.5	0	4.94 ± 0.01
	40	0.08 ± 0.00	12.4 ± 0.3	0	6.12 ± 0.01
	50	0.08 ± 0.00	14.3 ± 1.0	0	7.01 ± 0.00
1,000	10	0.07 ± 0.00	5.6 ± 0.3	0	2.19 ± 0.00
	20	0.11 ± 0.00	8.8 ± 0.2	0	2.93 ± 0.00
	30	0.12 ± 0.00	11.0 ± 0.5	0	3.71 ± 0.00
	40	0.12 ± 0.00	12.6 ± 0.4	0	4.54 ± 0.00
	50	0.13 ± 0.00	14.6 ± 0.1	0	5.47 ± 0.00
1,500	10	0.08 ± 0.01	5.5 ± 0.4	0	2.60 ± 0.00
	20	0.11 ± 0.00	7.5 ± 0.3	0	3.60 ± 0.00
	30	0.12 ± 0.01	9.3 ± 1.3	0	4.69 ± 0.01
	40	0.13 ± 0.02	10.4 ± 1.2	0	5.75 ± 0.00
	50	0.15 ± 0.01	13.6 ± 1.0	0	6.77 ± 0.00
2,000	10	0.08 ± 0.00	4.6 ± 0.2	0	2.95 ± 0.00
	20	0.11 ± 0.01	6.7 ± 0.9	0	4.20 ± 0.00
	30	0.13 ± 0.02	8.6 ± 1.4	0	5.47 ± 0.00
	40	0.13 ± 0.02	10.3 ± 1.2	0	6.65 ± 0.01
	50	0.12 ± 0.02	10.6 ± 1.2	0	7.73 ± 0.00

[a]The buffer used was MTE buffer. [b]The value was fixed to zero during fitting since it was negligibly small.

Chapter IV

Discussions

As shown in this study, structure, stability, and function of HjDHFR P1 were significantly affected by the addition of NaCl, indicating clear halophilic behaviors. The search for the mechanism of these halophilic characteristics could provide novel knowledge for understanding the interactions between proteins and small molecules in solution and the molecular adaptation mechanisms of enzymes to extreme environments.

IV-1. Halophilic mechanism of the structure of HjDHFR P1

As shown in Figs. III-3A and III-4B, the addition of NaCl ranging from 0 to 500 mM induced significant structural change to the HjDHFR P1 protein. Such structural change also occurred by lowering the pH to 6.0 (Fig. III-3B) or adding NADPH (Fig. III-6C). Since almost the same CD spectra were observed after these structural changes, it reflects the same structural change. Although the addition of salt or a ligand and lowering the pH might have different effects on the protein, the perturbation of hydration structures, induction of specific internal interactions, and reduction of repulsive forces between charged groups, all induced the same structural change to HjDHFR P1. Therefore, this structure would be the most stable conformation under physiological conditions, and HjDHFR P1 forms this conformation regardless of the type of stabilizing effect. Such conformational identity was also observed for the acid and thermal unfolding processes of EcDHFR (Ohmae et al. 1996).

Conversely, the addition of folate had no effect on the CD spectra of HjDHFR P1 in both the absence and presence of NaCl, although both spectra were clearly different (Fig.

III-6A and III-6B). These results suggested the following two possibilities: (1) HjDHFR P1 did not bind folate in the absence of NaCl, but the binding site was already formed at 500 mM NaCl; and (2) the observed change of the CD spectra was regardless of the structure of the binding site for folate, and the binding site was preserved without relation to NaCl concentration. Since the initial enzymatic activity was very law when enzyme-DHF solution without NaCl was mixed with the NADPH solution containing NaCl (Fig. III-11B), and the change in fluorescence due to rapid binding of DHF was very small in the absence of NaCl (Fig. III-12A), it is presumable that the binding site for folate was not formed in the absence of NaCl. Therefore, HjDHFR P1 has a partial structure which can binds to NADPH, and the addition of NaCl or the binding of NADPH induced structural formation of the substrate-binding site, coincident with the former possibility. This hypothesis was also supported by the results of the urea-induced unfolding experiments, which suggested the existence of a partial structure in HjDHFR P1 in the absence of NaCl and urea (Fig. III-8A).

IV-2. Halophilic mechanism of the structural stability of HjDHFR P1

As we reported previously (Ohmae et al. 2013b), equilibrium unfolding of typical small proteins such as DHFR follows a two-state unfolding process, which does not mean "two structures" or "two conformations," like the liquid–vapor equilibrium of n-hexane. When chain length increases to heptane or octane, the number of conformations acceptable for each molecule in both the liquid and vapor phases is increased dramatically, but the number of states is not increased. In addition, the Gibbs free energy change between both states, which is called "vaporization free energy", depends on intermolecular interactions between each molecule and not on intramolecular interactions.

In the case of protein unfolding, the number of states is also independent of the chain length of the protein, although the number of acceptable conformations in the unfolded state is significantly (and those in the native state may be somewhat) dependent on chain length. Furthermore, the Gibbs free energy change between both states, the so-called "protein stability", depends on intermolecular interactions.

Since protein unfolding experiments are usually conducted at low protein concentrations to avoid the contribution of protein–protein interactions, such intermolecular interactions mainly exist between the protein and water (and/or salt ions, in the case of halophilic proteins). Although the increased surface acidic residue content of halophilic proteins is a comprehensible feature showing different intermolecular interactions between the protein and water or salt ions from normal proteins, HjDHFR P1 probably employs another mechanism to change its intermolecular interactions because its acidic residue content is lower than that of EcDHFR (Fig. I-1).

As shown in Figs. III-7A and III-8A, the HjDHFR P1 protein was stabilized for both thermal- and urea-induced unfolding by the addition of NaCl. However, the NaCl concentration dependence of the thermodynamic parameters for both types of unfolding showed different tendencies. The parameters for thermal unfolding, T_m, ΔH_m, and ΔC_p, have a tendency to converge to constant values. Particularly, ΔC_p converged to 8.7 ± 0.2 $kJ \cdot mol^{-1} \cdot K^{-1}$ at over 500 mM NaCl (Fig. III-7B), which was consistent with the termination of structural formation (Fig. III-4B). Since ΔC_p is related to the solvent accessible surface exposed by protein unfolding, it is reasonable that ΔC_p depended on structural formation and was independent of the salt concentration in the range that the structure had already formed. Conversely, the increase of the T_m value at more than 500 mM NaCl might be associated with the stabilization of the unfolded state suggested by

the decrease of molar ellipticity at 80°C in Fig. III-7A. ΔH_m could be increased at more than 500 mM NaCl with the increase of T_m, since it is the enthalpy change at T_m. T_m and ΔH_m seem to saturate to constant values at a slightly higher salt concentration than 1,000 mM (Fig. III-7B).

On the contrary, the thermodynamic parameters for urea-induced unfolding, ΔG^o_u and C_m, depended linearly on NaCl concentration, and increased continuously over 500 mM (Fig. III-8B). Therefore, this stabilization effect could not be explained by structural formation. Such a linear increase in structural stability by salt was also observed for the urea-induced unfolding of EcDHFR and two HvDHFRs (Wright et al. 2002). Since ΔG_u values due to urea-induced unfolding contain chemical potential changes of urea and hydrated water, as we described previously (Ohmae et al. 2013b), and salt can affect the chemical potential of these components, the results of these experiments suggested the contribution of preferential interactions between proteins and salt ions to the structural stability of DHFRs.

IV-3. Halophilic mechanism of the enzymatic function of HjDHFR P1

As shown in Fig. III-10, the optimal NaCl concentration for HjDHFR P1 activity at pH 8.0, 250 mM, was different from that for full structural formation, 500 mM (Fig. III-4B). Moreover, the enzyme was also activated by the addition of NaCl at pH 6.0 under saturated concentrations of NADPH, although these conditions induced structural formation in the absence of NaCl (Figs. III-3B and III-6C). Therefore, the effects of salt ions on the enzymatic activity of HjDHFR P1 are independent from structural formation. However, the further addition of NaCl decreased enzymatic activity, indicating additional effects of salt ions. Such an observation is confusing because the same salt has opposite

effects on the same enzyme depending on its concentration. However, the steady-state turnover of enzymes contains various enzyme-ligand complexes and multiple steps between them. Therefore, salt can affect the equilibria and reaction rates for these complexes in different ways, and the population of the complexes and the rate-determining step of enzyme turnover can be changed depending on the salt concentration, resulting in the inversion of the apparent effect of salt on activity. One of the purpose of this study was to clarify such activation and inactivation mechanisms on the enzyme activity of HjDHFR P1 by salt, and discuss them in comparison with those of other halophilic DHFRs: HvDHFR 1 and 2, and non-halophilic EcDHFR.

IV-3-1. The analysis of salt-binding models

The simplest mechanism to explain the biphasic behavior of HjDHFR P1 activity (Fig. III-10) is the reversible specific binding of two salt ions, in which one has activation effects while the other has inactivation effects (Scheme IV-1). In this scheme, the total enzyme concentration, $[E]_t$, can be divided into four components: the concentration of salt-free enzyme ([E]), the activated enzyme by the binding of salt ions ([EA]), and the inactivated enzyme by the binding of salt ions, ([EB]) and ([EAB]).

$$[E]_t = [E] + [EA] + [EB] + [EAB] \qquad (IV-1)$$

To simplify the theoretical equation, I assumed that the salt ions bind to the enzyme in a one-to-one ratio, and the dissociation constants between them, K_{dA} and K_{dB}, are independent of each other as follows:

$$K_{dA} = \frac{[E][A]}{[EA]} = \frac{[EB][A]}{[EAB]} \qquad (IV-2)$$

$$K_{dB} = \frac{[E][B]}{[EB]} = \frac{[EA][B]}{[EAB]} \qquad (IV-3)$$

The total salt ion concentration, $[A]_t$ and $[B]_t$, is equal to the salt concentration for univalent salts, although either cations or anions can correspond to the salt ions, A and B. The free salt ion concentration, [A] and [B], can be regarded as equal to the total salt ion concentration, $[A]_t$, because the salt concentration is 10^6-fold higher than that of the enzyme in this experiment, and the decrease of the free salt ion concentration by binding to the enzyme is negligible.

$$[\mathrm{A}] = [\mathrm{B}] = [\mathrm{A}]_t \qquad (\mathrm{IV}-4)$$

Finally, it was assumed that the enzymatic activity of the inactivated species (EB and EAB) is negligible compared to that of the other enzyme species (E and EA), since the kinetic constants of the enzymatic reaction catalyzed by these species usually represent negative values by fitting. In this assumption, the observed initial velocity of the enzyme reaction, V, is expressed as follows:

$$V = k_{\mathrm{E}}[\mathrm{E}] + k_{\mathrm{EA}}[\mathrm{EA}] \qquad (\mathrm{IV}-5)$$

where k_{E} and k_{EA} are kinetic constants of the enzymatic reaction catalyzed by the E and EA species, respectively. The combination of eqs. IV-1 to IV-5 gives the following equation:

$$V = \left(k_{\mathrm{E}} + \frac{k_{\mathrm{EA}}[\mathrm{A}]_{\mathrm{t}}}{K_{\mathrm{dA}}}\right)\left\{\frac{K_{\mathrm{dA}}K_{\mathrm{dB}}[\mathrm{E}]_{\mathrm{t}}}{(K_{\mathrm{dA}} + [A]_{\mathrm{t}})(K_{\mathrm{dB}} + [A]_{\mathrm{t}})}\right\} \qquad (\mathrm{IV}-6)$$

However, the theoretical curve derived from this hypothesis did not fit the experimental data, especially at high salt concentrations (Fig. IV-1 and Table IV-1). Besides, the inactivation profile at high NaCl concentrations shown in Fig. III-10 does not follow a hyperbolic curve but follows an exponential curve. Therefore, the activation process can be explained by the reversible binding of salt ions, but the inactivation process cannot.

Next, I considered the second mechanism, which includes activation by the reversible

specific binding of a salt ion to the enzyme, and inactivation by an irreversible process such as modification by salt ions or aggregation of the enzyme (Scheme IV-2). The inactivation profile follows an exponential curve in this hypothesis.

$$\frac{\mathrm{d}([\mathrm{E}]+[\mathrm{EA}])}{\mathrm{dt}} = -k_{\mathrm{B}}([\mathrm{E}]+[\mathrm{EA}])[\mathrm{B}] \qquad (\mathrm{IV}-7)$$

$$([\mathrm{E}]+[\mathrm{EA}] = [\mathrm{E}]_{\mathrm{t}} \ \ at \ \ t = 0)$$

The combination of eqs. IV-1, IV-2, IV-4, IV-5, and IV-7 gives the following equation:

$$V = \left(k_{\mathrm{E}} + \frac{k_{\mathrm{EA}}[\mathrm{A}]_{\mathrm{t}}}{K_{\mathrm{dA}}}\right)\left\{\frac{K_{\mathrm{dA}}[\mathrm{E}]_{\mathrm{t}}\exp(-k_{\mathrm{B}}[\mathrm{A}]_{\mathrm{t}}t)}{K_{\mathrm{dA}}+[\mathrm{A}]_{\mathrm{t}}}\right\} \qquad (\mathrm{IV}-8)$$

The theoretical curve derived from this hypothesis fitted the experimental data (Fig. IV-2 and Table IV-2). However, enzymatic activity must depend on the pre-incubation time with salt in this hypothesis, although it was shown to be independent (Fig. IV-2). Besides, dilution of the salt concentration fully returned the activity of HjDHFR P1 (data not shown). Therefore, the inactivation process should be explained by some kind of reversible process.

Then, I considered the third mechanism, which includes activation by reversible specific salt binding and inactivation by structural stabilization associated with conformational or dynamics changes induced by preferential interactions between salt ions and the enzyme (Scheme IV-3). In this scheme, the total enzyme concentration, $[\mathrm{E}]_{\mathrm{t}}$, can be divided into four components: the concentration of non-stabilized free enzyme ([E]), the enzyme species stabilized by preferential interactions with salt ions ([E′]), the activated enzyme by the binding of salt ions ([EA]), and the stabilized enzyme bound to salt ions ([E′A]).

$$[\mathrm{E}]_{\mathrm{t}} = [\mathrm{E}]+[\mathrm{E}']+[\mathrm{EA}]+[\mathrm{E}'\mathrm{A}] \qquad (\mathrm{IV}-9)$$

To simplify the theoretical equation, I assumed that the salt ions bind to the enzyme

in a one-to-one ratio, and the dissociation constant between them, K_{dA}, is independent of the stabilization effect as follows:

$$K_{dA} = \frac{[E][A]}{[EA]} = \frac{[E'][A]}{[E'A]} \qquad (IV-10)$$

The total salt ion concentration, $[A]_t$ is equal to the salt concentration for univalent salts, and the free salt ion concentration, [A], can be regarded as equal to the total salt ion concentration, $[A]_t$, as mentioned above (eq. IV-4).

I also assumed that the equilibrium constant between non-stabilized and stabilized enzyme species, K_s, is independent of salt ion binding, and the Gibbs free energy change due to stabilization, ΔG_s, depended linearly on the salt concentration as follows:

$$K_S = \frac{[E']}{[E]} = \frac{[E'A]}{[EA]} \qquad (IV-11)$$

$$\Delta G_S = -RT \ln K_S = \Delta G_S^o - m_S[A]_t \qquad (IV-12)$$

where $\Delta G°_s$ and m_s are the Gibbs free energy change in the absence of salt and the salt concentration dependence of ΔG_s, respectively.

Finally, it was assumed that the enzymatic activity of the stabilized enzyme species (E′ and E′A) is negligible compared to that of the other enzyme species (E and EA) as mentioned above (eq. IV-5). The combination of eqs. IV-4, IV-5, IV-9, IV-10, IV-11, and IV-12 gives the following equation:

$$V = \frac{(k_E + k_{EA}[A]_t/K_{dA})[E]_t}{[1 + \exp\{-(\Delta G_S^o - m_S[A]_t)/RT\}](1 + [A]_t/K_{dA})} \qquad (IV-13)$$

The theoretical curve derived from this equation was well-fitted to the experimental data, as shown in Fig. III-10, and the obtained parameters are listed in Table IV-3. The obtained K_{dA} and k_{EA} values at pH 6.0, 146 ± 14 mM and 43.8 ± 24.8 s^{-1}, respectively, were 6.6- and 3.9-fold larger than those at pH 8.0, 22 ± 6 mM and 11.3 ± 1.6 s^{-1}, respectively, indicating that the specific binding effect was strongly pH-dependent.

However, the obtained $\Delta G°_s$ and k_E values at pH 6.0 and 8.0 were coincident within the estimation errors, approximately –2.0 kJ·mol^{-1} and 3.0 s^{-1}, respectively, indicating that the effects of preferential interaction were almost pH-independent from pH 6.0–8.0. Considering the estimation errors of the obtained fitting parameters, a more complicated scheme could not be applied to the present experimental data. However, the results strongly suggested that preferential interactions between the protein and salt ions contribute to the inactivation process of HjDHFR P1.

IV-3-2. Activation mechanism of HjDHFR P1 by salt

As discussed in the previous section, activation of HjDHFR P1 by salt could be explained by the binding of salt ions. From a comparison of the effects of inorganic and organic cations and anions, it is obvious that chloride anions enhance the enzymatic activity of HjDHFR P1 (inset of Fig. III-10). Furthermore, the hyperbolic activation effects against salt concentration shown in the insets of Fig. III-11 indicated that anion binding was crucial. Although anion can bind to both the enzyme and substrate, the effective binding is occurred on the enzyme or enzyme-ligand complexes since the activation effect was observed in the saturated substrates condition. However, there are two possibilities for such an activation mechanism induced by anion binding: (1) acceleration of the rate-determining step in the catalytic cycle, and (2) population change of the inactive (or low-activity) and active (or high-activity) conformers caused by the equilibrium shift between them.

The steady-state enzymatic turnover of DHFR includes at least five steps: two binding steps of NADPH and DHF, hydride transfer from NADPH to DHF, and two releasing steps of $NADP^+$ and THF. From the sufficiently small K_m values observed in the steady-

state kinetics experiments, the two binding steps can be eliminated as candidates for the rate-determining step (Table III-6). The constant enzyme activity (Fig. III-10) and full isotope effects (Table III-5) at pH 10.0 indicate that the hydride-transfer rate is independent of salt concentration, and the activation mechanism affects the rate-determining step at the neutral pH region. In addition, from the rapid-phase ligand binding experiments, the binding rates of DHF and NADPH to HjDHFR P1 and the releasing rate of THF from the enzyme were not accelerated by salt (Table III-8). Although I could not measure the $NADP^+$-releasing rate, the difficulty of this measurement suggested a rapid reaction rate for this process and low probability that this step was the rate-determining step. Therefore, mechanism (1) seems improbable.

Conversely, when the enzymatic reaction was initiated by mixing the enzyme–DHF solution without salt to the NADPH solution containing salt, the initial activity of HjDHFR P1 was low and increased gradually as the reaction progressed (Fig. III-11B). In addition, the amplitude of fluorescence quenching by the rapid binding of DHF clearly increased with increasing salt concentration (inset of Fig. III-12A). These results indicate that DHF cannot bind to HjDHFR P1 before the anion binds to the enzyme. Therefore, mechanism (2), population change of the anion-bound and anion-unbound enzyme conformers, which are binding-competent and -incompetent forms for DHF, respectively, is a reasonable explanation for the activation mechanism of HjDHFR P1 by salt, although the secondary structure of HjDHFR P1 is already formed in the absence of salt at pH 6.0 (Fig. III-3B).

Such ligand binding-competent and -incompetent conformers are also observed for EcDHFR as E1 and E2, respectively (Cayley et al. 1981). In the case of EcDHFR, the exponential phase shown in the rapid-phase fluorescence quenching reflects the binding

of NADPH, DHF, or folate to the E1 conformer, and the subsequent linear phase reflects interconversion from E2 to E1. Since the binding of NADPH to HjDHFR P1 showed similar exponential and linear phases (Table III-7), it is possible that the latter phase reflects the interconversion of the binding-competent and -incompetent conformers. However, such interconversion could be negligible for the salt concentration dependence of the enzyme activity shown in Fig. III-10, because I pre-incubated the enzyme with NADPH for 10 min, and the pre-incubation from 5 to 20 min showed almost the same results. Conversely, binding of DHF to HjDHFR P1 showed only single exponential phase suggesting that interconversion between DHF binding-competent and -incompetent conformers seems hardly occurred without salt, although additional measurements in longer time scale are needed.

IV-3-3. Inactivation mechanism of HjDHFR P1 by salt

As discussed above, the activation mechanism of HjDHFR P1 by salt could be explained by the population change of the active and inactive forms of the enzyme. Thus, the rate-determining step of enzyme turnover need not change according to salt concentration. Therefore, it is presumable that the rate-determining step at the neutral pH region is the THF-releasing step, as for EcDHFR, and the rate of this step was decelerated by salt. The consistency between the k_{cat} and k_{off} values for THF confirms this presumption (Tables III-6 and III-8). As discussed in the section IV-3-1, preferential interactions between the protein and salt ions contributed to the inactivation profile of HjDHFR P1. The deceleration of the THF-releasing step is consistent with this observation.

IV-3-4. Salt effects on the elementary steps of the enzymatic reaction of HjDHFR P1

From the experimental results of this study, I summarized the salt effects on the elementary steps of the enzymatic reaction of HjDHFR P1 as shown in Scheme IV-4. Anion-unbound enzyme (E) and anion-bound enzyme (EA) are in equilibrium in solution. The NADPH-binding rate for the former conformer is more rapid than for the latter one. DHF can bind only to the latter conformer, but the reaction rate is salt-concentration independent. During steady-state turnover, hydride transfer from NADPH to DHF, which is the rate-determining step at the basic pH region, is independent of salt concentration. In addition, the THF-releasing step, which is the rate-determining step at the neutral pH region, is decelerated by salt. Although anion-unbound enzyme can create another catalytic cycle, the catalytic efficiency of this conformer is very low compared with the anion-bound conformer and it can be ignored as assumed in the section IV-3-1.

IV-4. Comparison with other DHFRs

It is noteworthy that the activation mechanism of HjDHFR P1 is consistent with previous results for other halophilic DHFRs (i.e., HvDHFR 1 and 2). Salt induces the structural formation of both HvDHFRs resulting in an enhancement of their enzymatic activity (Wright et al. 2002). The equilibrium and kinetic stability studies of HvDHFR 1 show that structural formation indicates a population increase of the number of folded molecules caused by destabilization of the unfolded state (Gloss et al. 2008). However, the stabilizing effect of salt is not specific for halophilic enzymes; the same effect is also observed for EcDHFR (Wright et al. 2002).

In addition, the structural formation of HvDHFR 1 is almost complete at 1 M KCl, as determined by monitoring CD and fluorescence spectra, although it is activated

monotonously up to 3.5 M KCl (Wright et al. 2002). Thus, HvDHFR 1 should have another activation mechanism. Blecher et al. (1993) reported that the K_m value for DHF is decreased by 10-fold from 0.9 to 0.08 mM as KCl concentration increases from 0.5 to 3.0 M, indicating the enhancement of the affinity between DHF and HvDHFR 1. Such an observation can be explained by the existence of binding-competent and -incompetent conformers for DHF. Conversely, HvDHFR 2 shows similar salt concentration-dependence of enzyme activity to HjDHFR P1, with a maximum at 500 mM and gradual decrease by the further addition of KCl (Ortenberg et al. 2000). Although the detailed activation and inactivation mechanisms are not clear, the same mechanisms can be presumed.

Since the rate-determining step of EcDHFR at the neutral pH region is the THF-releasing step, EcDHFR should also show a similar salt inactivation profile to HjDHFR P1. However, according to previous reports, the enzymatic activity of EcDHFR is markedly decreased as NaCl concentration increases (Baccanari et al. 1975, Ohmae et al. 2013a). This is caused by the binding of an inorganic cation near the substrate-binding cleft, which was confirmed by NMR experiments. Although inorganic cations strongly inhibit the enzyme activity of EcDHFR, TMACl, which has an organic cation, induces a gradual decrease of its activity, an approximately 30% reduction from 0 to 500 mM at pH 8.0, consistent with the inactivation effect of NaCl on HjDHFR P1 (Ohmae et al. 2013a). Therefore, deceleration of the THF-releasing rate by salt may be a common feature of both DHFRs, and HjDHFR P1 may have maximum activity in the absence of salt if the population change of the active conformer has not occurred.

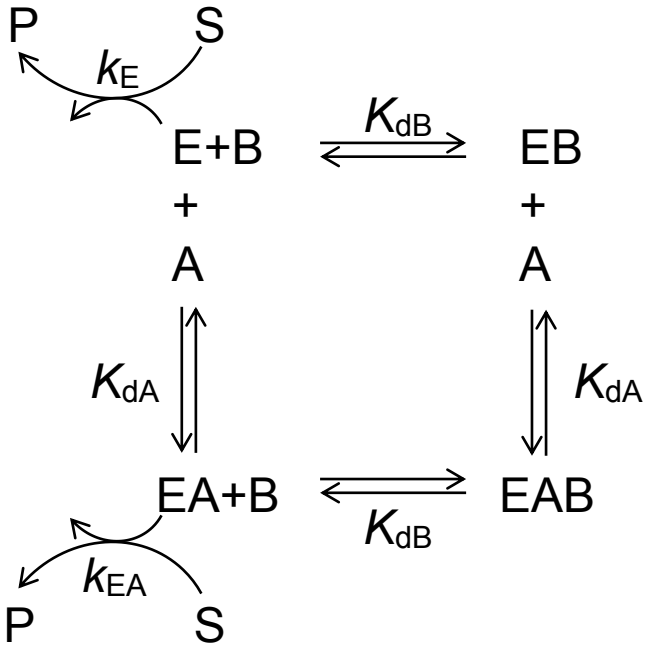

Scheme IV-1. Scheme for the effects of salt ions on the enzymatic activity of HjDHFR P1, including activation and inactivation by the reversible binding of salt ions. E is the free enzyme species. A and B are salt ions, and EA and EB are the corresponding enzyme species that bound each salt ion, respectively. K_{dA} and K_{dB} are the dissociation constants for the corresponding salt ion binding. k_E and k_{EA} are the kinetic constants of the enzymatic reaction for the E and EA species, respectively. S and P indicate the substrate and product, respectively. The initial velocity of the enzymatic reaction is represented as eq. IV-6 according to this scheme.

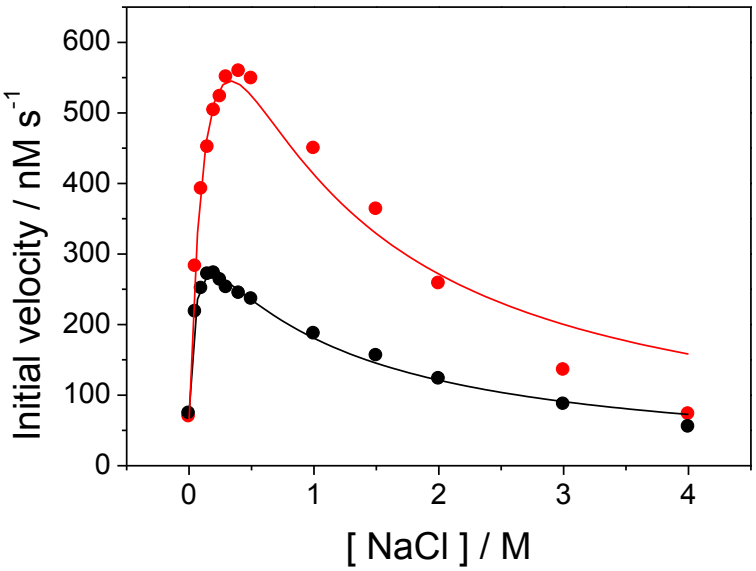

Fig. IV-1. Curve fitting for the NaCl concentration dependence of the enzymatic activity of HjDHFR P1 at 25°C and pH 6.0 (red) and pH 8.0 (black) by eq. IV-6.

Table IV-1. Obtained fitting parameters for the NaCl concentration dependence of HjDHFR P1 activity using eq. IV-6 derived from scheme IV-1.

Parameter	pH 8.0	pH 6.0
K_{dA} / mM	54 ± 11	353 ± (1.7×10^6)
K_{dB} / mM	914 ± 104	353 ± (1.7×10^6)
k_E / s^{-1}	0.90 ± 0.09	0.75 ± 0.43
k_{EA} / s^{-1}	4.76 ± 0.29	25.51 ± (1.2×10^5)

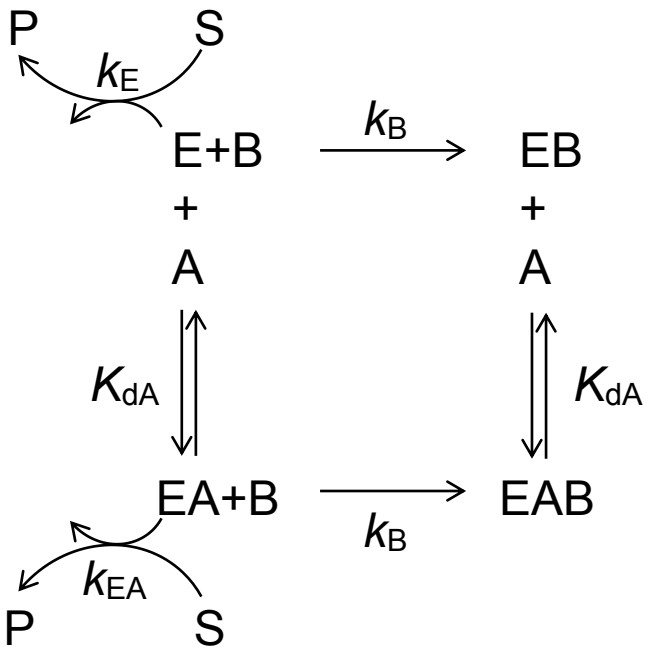

Scheme IV-2. Scheme for the effects of salt ions on the enzymatic activity of HjDHFR P1, including activation by the reversible binding of a salt ion and inactivation by an irreversible process such as modification by salt ions or aggregation of the enzyme. Since the activity is lost by the structural change of the enzyme before aggregation, aggregated species such as En are not necessary in this scheme. k_B is the kinetic constant of the irreversible binding of salt ions B. Other abbreviations are the same as scheme IV-1. The initial velocity of the enzymatic reaction is represented as eq. IV-8 according to this scheme.

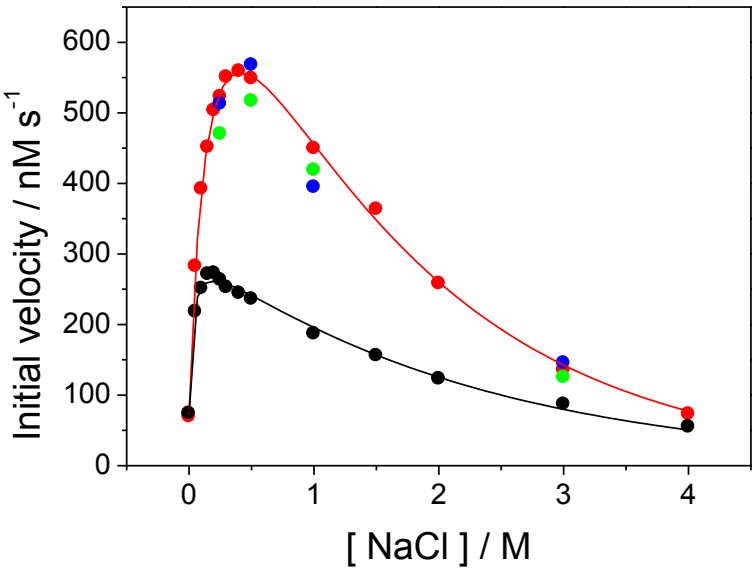

Fig. IV-2. Curve fitting for the NaCl concentration dependence of the enzymatic activity of HjDHFR P1 at 25°C and pH 6.0 (red) and pH 8.0 (black) for a pre-incubation of 10 min by eq. IV-8. Observed activities for different pre-incubation times (5 and 20 min) at pH 6.0 are also shown by blue and green, respectively.

Table IV-2. Obtained fitting parameters for the NaCl concentration dependence of HjDHFR P1 activity using eq. IV-8 derived from scheme IV-2.

Parameter	pH 8.0	pH 6.0
K_{dA} / mM	27 ± 5	165 ± 11
$k_B \times 10^4$ / min^{-1}	4.6 ± 0.2	6.3 ± 0.2
k_E / s^{-1}	0.89 ± 0.09	0.88 ± 0.09
k_{EA} / s^{-1}	3.79 ± 0.10	11.80 ± 0.31

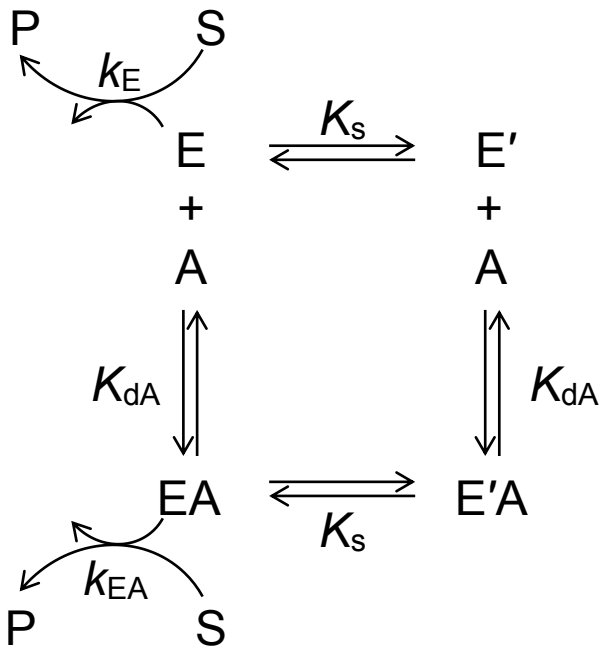

Scheme IV-3. Predicted scheme for the effects of salt ions on the enzymatic activity of HjDHFR P1. E and E′ are enzyme species that are non-stabilized and stabilized by preferential interactions between the enzyme and salt ions, respectively, and EA and E′A are the corresponding enzyme species bound by a salt ion, A, respectively. K_s is the equilibrium constant between the non-stabilized and stabilized enzyme species. Other abbreviations are the same as scheme IV-1. The initial velocity of the enzymatic reaction is represented as eq. IV-13 according to this scheme.

Table IV-3. Obtained fitting parameters for the NaCl concentration dependence of HjDHFR P1 activity at 25°C using eq. IV-13 derived from scheme IV-3.

Parameter	pH 8.0	pH 6.0
K_{dA} / mM	22 ± 6	146 ± 14
$\Delta G°_s$ / kJ·mol^{-1}	–1.8 ± 0.5	–2.7 ± 1.7
m_s / J·mol^{-1}·mM^{-1}	1.4 ± 0.1	1.7 ± 0.1
k_E / s^{-1}	2.6 ± 0.3	3.4 ± 1.9
k_{EA} / s^{-1}	11.3 ± 1.6	43.8 ± 24.8

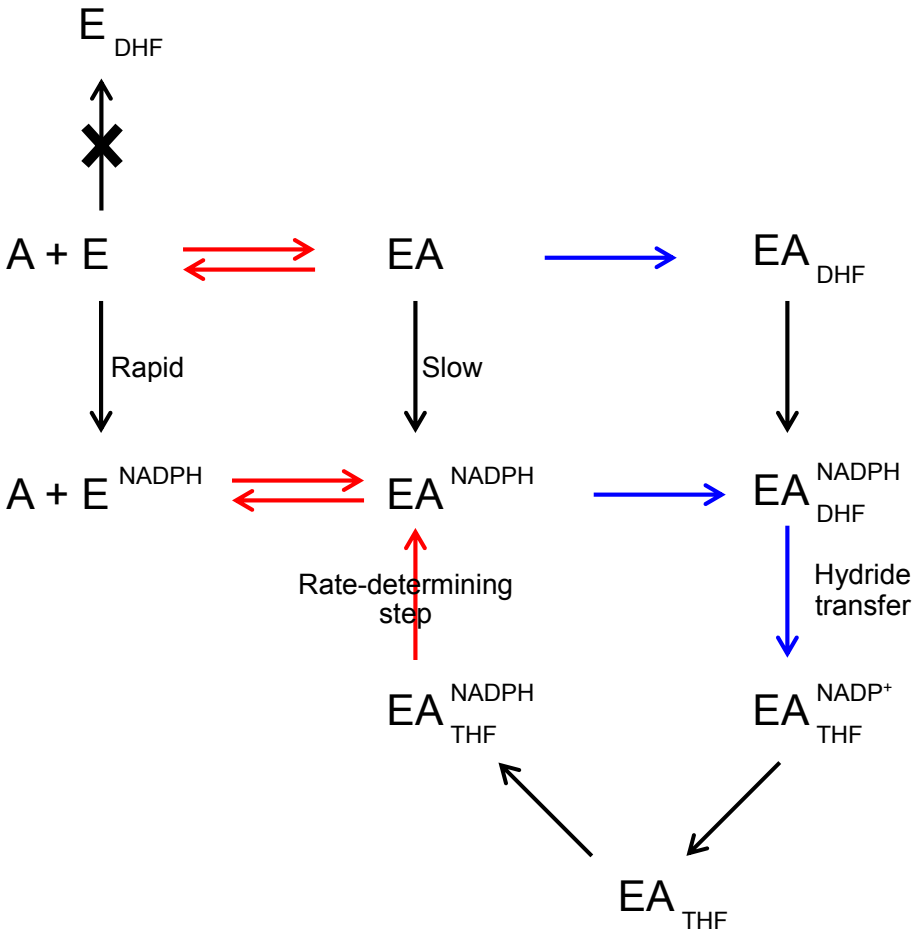

Scheme IV-4. Schematic drawing of the effects of salt on the elementary steps of the enzymatic reaction of HjDHFR P1 at the neutral pH region. E and EA indicate the anion-unbound and anion-bound conformers, respectively. The red and blue arrows indicate salt concentration-dependent and -independent processes, respectively.

Chapter V

Conclusions

A novel DHFR from an extremely halophilic archaeon *Haloarcula japonica* strain TR-1, HjDHFR P1, was successfully overexpressed and purified. Firstly, to elucidate how salt ions affect the structure of HjDHFR P1, its secondary and tertiary structures were analyzed by CD and fluorescence spectra, respectively. Experimental results suggested that the addition of 500 mM NaCl induced the formation of the substrate-binding site in HjDHFR P1. However, its structural stability for the thermal and urea-induced unfolding increased depending on NaCl concentration regardless of this structural change, and the halophilic mechanism is suggested as the contribution of preferential interactions between the protein and salt ions.

On the other hand, HjDHFR P1 shows moderately halophilic characteristics for enzymatic activity at pH 6.0, although there are no significant effects of NaCl on its secondary structure. pH and salt concentration dependencies showed that this enzyme was activated at the acidic to neutral pH region, but not activated at the basic pH region, in which the rate-determining step was the hydride-transfer step. Besides, rapid-phase ligand binding experiments using stopped-flow fluorescence quenching showed that the amplitude of the rapid binding of DHF to HjDHFR P1 increased with increasing NaCl concentration at pH 6.0, although the reaction rate was almost constant. In addition, the THF-releasing rate decreased with increasing NaCl concentration, consistent with the decrease of the k_{cat} value. These results suggested that the activation mechanism of HjDHFR P1 by salt is the population change of anion-unbound and anion-bound conformers, which are binding-incompetent and -incompetent forms for DHF,

respectively. On the other hand, the salt-inactivation mechanism is *via* deceleration of the THF-releasing rate, which is the rate-determining step at the neutral pH region.

Thus, HjDHFR P1 had halophilic characteristics in its structure, stability, and enzymatic function, although its predicted backbone structure almost overlapped with that of the non-halophilic DHFR from *Escherichia coli*, EcDHFR. And the activation mechanisms of structure, stability, and function of this enzyme may also be possible for other halophilic DHFRs—DHFR from *Haloferax volcanii* (HvDHFR 1 and 2)—and the inactivation mechanism in its function may be a common feature of non-halophilic EcDHFR.

References

Allers T (2010) Overexpression and purification of halophilic proteins in *Haloferax volcanii*. Bioengineered Bugs 1: 288−290.

Arakawa T, Timasheff SN (1984) Mechanism of protein salting in and salting out by divalent cation salts: Balance between hydration and salt binding. Biochemistry 23: 5912−5923.

Baccanari D, Phillips A, Smith S, Sinski D, Buchall J (1975) Purification and properties of *Escherichia coli* dihydrofolate reductase. Biochemistry 14: 5267−5273.

Baccanari DP, Averett D, Briggs C, Burchall J (1977) *Escherichia coli* dihydrofolate reductase: Isolation and characterization of two isozymes. Biochemistry 16:3566–3572.

Binbuga B, Boroujerdi AFB, Young JK (2007) Structure in an extreme environment: NMR at high salt. Protein Sci. 16: 1783−1787.

Behiry EM, Evans RM, Guo J, Loveridge EJ, Allemann RK (2014) Loop interactions during catalysis by dihydrofolate reductase from *Moritella profunda*. Biochemistry 53:4769–4774.

Blecher O, Goldman S, Mevarech M (1993) High expression in *Escherichia coli* of the gene coding for dihydrofolate reductase of the extremely halophilic archaebacterium *Haloferax volcanii*. Reconstitution of the active enzyme and mutation studies. Eur. J. Biochem. 216: 199−203.

Boroujerdi AFB, Young JK (2009) NMR-derived folate-bound structure of dihydrofolate reductase 1 from the halophile *Haloferax volcanii*. Biopolymers 91:140–144.

Cameron CE, Benkovic SJ (1997) Evidence for a functional role of the dynamics of glycine-121 of *Escherichia coli* dihydrofolate reductase obtained from kinetic analysis

of a site-directed mutant. Biochemistry 36:15792–15800.

Cayley PJ, Dunn SM, King RW (1981) Kinetics of substrate, coenzyme, and inhibitor binding to *Escherichia coli* dihydrofolate reductase. Biochemistry 20: 874–879.

Chen J, Taira K, Tu CD, Benkovic SJ (1987) Probing the functional role of phenylalanine-31 of *Escherichia coli* dihydrofolate reductase by site-directed mutagenesis. Biochemistry 26:4093–4100.

Danson MJ, Hough DW (1997) The structural basis of protein halophilicity. Comp. Biochem. Phisiol. A Physiol. 117: 307−312.

David CL, Howell EE, Farnum MF, Villafranca JE, Oatley SJ, Kraut J (1992) Structure and function of alternative proton-relay mutants of dihydrofolate reductase. Biochemistry 31:9813–9822.

Dias CL, Ala-Nissila T, Wong-ekkabut J, Vattulainen I, Grant M, Kattunen M (2010) The hydrophobic effect and its role in cold denaturation. Cryobiology 60: 91−99.

Fierke CA, KJohnson KA, Benkovic SJ (1987) Construction and evaluation of the kinetic scheme associated with dihydrofolate reductase from *Escherichia coli*. Biochemistry 26: 4085−4092.

Fierke CA, Benkovic SJ (1989) Probing the functional role of threonine-113 of *Escherichia coli* dihydrofolate reductase for its effect on turnover efficiency, catalysis, and binding. Biochemistry 28:478–486.

Garvey EP, Matthews CR (1989) Effects of multiple replacements at a single position on the folding and stability of duhydrofolate reductase from *Escherichia coli*. Biochemistry 28:2083–2093.

Gloss LM, Topping TB, Binder AK, Lohman JR (2008) Kinetic folding of *Haloferax volcanii* and *Escherichia coli* dihydrofolate reductases: Haloadaptation by unfolded

state destabilization at high ionic strength. J. Mol. Biol. 376: 1451−1462.

Grubbs J, Rahmanian S, DeLuca A, Padmashali C, Jackson M, Duff MR Jr., Howell E (2011) Thermodynamics and solvent effects on substrate and cofactor binding in *Escherichia coli* chromosomal dihydrofolate reductase. Biochemistry 50:3673–3685.

Gulevsky AK, Relina LI (2013) Molecular and genetic aspects of protein cold denaturation. Cryo Letters 34: 62−82.

Guo J, Luk LYP, Loveridge EJ, Allemann RK (2014) Thermal adaptation of dihydrofolate reductase from the moderate thermophile *Geobacillus stearothermophilus*. Biochemistry 53:2855–2863.

Hamamoto T, Takashina T, Grant WD, Horikoshi K (1988) Asymmetric cell division of a triangular halophilic archaebacterium. FEMS Microbiol. Lett. 56: 221−224.

Holzwarth G, Doty P (1965) Ultraviolet circular dichroism of polypeptides. J. Am. Chem. Soc. 87: 218−228.

Horikoshi K, Aono R, Nakamura S (1993) The triangular halophilic archaebacterium *Haloarcula japonica* strain TR-1. Experientia 49: 497−502.

Huennekens FM (1996) In search of dihydrofolate reductase. Protein Sci. 5: 1201−1208.

Ishibashi M, Hayashi T, Yoshida C, Tokunaga M (2013) Increase of salt dependence of halophilic nucleoside diphosphate kinase caused by a single amino acid substitution. Extremophiles 17: 585−591.

Jennings PA, Finn BE, Jones BE, Matthews CR (1993) A reexamination of the folding mechanism of dihydrofolate reductase from *Escherichia coli*: verification and refinement of a four-channel model. Biochemistry 32:3783–3789.

Karan R, Khare SK (2011) Stability of haloalkaliphilic *Geomicrobium* sp. protease modulated by salt. Biochemistry (Moscow) 76:840–848

Kuwajima K, Garvey EP, Finn BE, Matthews CR, Sugai S (1991) Transient intermediates in the folding of dihydrofolate reductase as detected by far-ultraviolet circular dichroism spectroscopy. Biochemistry 30:7693–7703.

Luk LYP, Loveridge EJ, Allemann RK (2014) Different dynamical effects in mesophilic and hyperthermophilic dihydrofolate reductases. J. Am. Chem. Soc. 136:6862–6865.

Madern D, Ebel C, Zaccai G (2000) Halophilic adaptation of enzymes. Extremophiles 4: 91−98.

Mevarech M, Frolow F, Gloss LM (2000) Halophilic enzymes: proteins with a grain of salt. Biophys. Chem. 86: 155−164.

Murakami C, Ohmae E, Tate S, Gekko K, Nakasone K, Kato C (2010) Cloning and characterization of dihydrofolate reductases from deep-sea bacteria. J. Biochem. 147: 591–599.

Murakami C, Ohmae E, Tate S, Gekko K, Nakasone K, Kato C (2011) Comparative study on dihydrofolate reductases from *Shewanella* species living in deep-sea and ambient atmospheric environments. Extremophiles 15: 165–175.

Nakamura S, Nakasone K, Takashina T (2011) Genetics and genomics of triangular disc-shaped halophilic archaeon *Haloarcula japonica* strain TR-1. In: Horikoshi K, Antranikian G, Bull A, Robb F, Stetler K (eds) Extremophiles Handbook. Springer-Verlag. Tokyo. pp 363−381.

Nishiyama Y, Takashina T, Grant WD, Horikoshi K (1992) Ultrastructure of the cell wall of the triangular halophilic archaebacterium *Haloarcula japonica* strain TR-1. FEMS Microbiol. Lett. 99:43–48.

Ohmae E, Kurumiya T, Makino S, Gekko K (1996) Acid and Thermal Unfolding of *Escherichia coli* Dihydrofolate Reductase. J. Biochem. 120: 946−953.

Ohmae E, Fukumizu Y, Iwakura M, Gekko K (2005) Effects of mutation at methionine-42 of *Escherichia coli* dihydrofolate reductase on stability and function: Implication of hydrophobic interactions. J. Biochem. 137: 643−652.

Ohmae E, Tatsuta M, Abe F, Kato C, Tanaka N, Kunugi S, Gekko K (2008) Effects of pressure on enzyme function of *Escherichia coli* dihydrofolate reductase. Biochim. Biophys. Acta 1784: 1115−1121.

Ohmae E, Murakami C, Tate S, Gekko K, Hata K, Akasaka K, Kato C (2012) Pressure dependence of activity and stability of dihydrofolate reductases of the deep-sea bacterium *Moritella profunda* and *Escherichia coli*. Biochim. Biophys. Acta 1824: 511−519.

Ohmae E, Miyashita Y, Tate S, Gekko K, Kitazawa S, Kitahara R, Kuwajima K (2013a) Solvent environments significantly affect the enzymatic function of *Escherichia coli* dihydrofolate reductase: Comparison of wild-type protein and active-site mutant D27E. Biochim. Biophys. Acta 1834: 2782−2794.

Ohmae E, Miyashita Y, Kato C (2013b) Thermodynamic and functional characteristics of deep-sea enzymes revealed by pressure effects. Extremophiles 17: 701−709.

Onodera M, Yatsunami R, Tsukimura W, Fukui T, Nakasone K, Takashina T, Nakamura S (2013) Gene analysis, expression, and characterization of an intracellular α-amylase from the extremely halophilic archaeon *Haloarcula japonica*. Biosci. Biotechnol. Biochem. 77: 281−288.

Oren A, Mana L (2002) Amino acid composition of bulk protein and salt relationships of selected enzymes of *Salinibacter ruber*, an extremely halophilic bacterium. Extremophiles 6: 217−223.

Ortega G, Lain A, Tadeo X, Lopez-Mendez B, Castano D, Millet O (2011) Halophilic

enzyme activation induced by salts. Scientific Report 10: 1−6.

Ortenberg R, Rozenblatt-Rosen O, Mevarech M (2000) The extremely halophilic archaeon *Haloferax volcanii* has two very different dihydrofolate reductases. Molecular Microbiology 35: 1493−1505.

Osborne MJ, Venkitakrishnan RP, Dyson HJ, Wright PE (2003) Diagnostic chemical shift markers for loop conformation and substrate and cofactor binding in dihydrofolate reductase complexes. Protein Sci. 12:2230–2238.

Ozawa K, Harashina T, Yatsunami R, Nakamura S (2005) Gene cloning, expression and partial characterization of cell division protein FtsZ1 from extremely halophilic archaeon *Haloarcula japonica* strain TR-1. Extremophiles 9: 281−288.

Pace CN (1985) Determination and analysis of urea and guanidine hydrochloride denaturation curves. Methods Enzymol. 131: 266−280.

Perry KM, Onuffer JJ, Touchette NA, Herndon CS, Gitteleman MS, Matthews CR, Chen JT, Mayer RJ, Taira K, Benkovic SJ, Howell EE, Kraut J (1987) Effects of single amino acid replacements on the folding and stability of dihydrofolate reductase from *Escherichia coli*. Biochemistry 26:2674–2682.

Pieper U, Kapadia G, Mevarech M, Herzberg O (1998) Structural features of halophilicity derived from the crystal structure of dihydrofolate reductase from the Dead Sea halophilic archaeon, *Haloferax volcanii*. Structure 6: 75−88.

Roesser M, Müller V (2001) Osmoadaptation in bacteria and archaea: common principles and differences. Environ. Microbiol. 3:743–754.

Sawaya MR, Kraut J (1997) Loop and subdomain movements in the mechanism of *Escherichia coli* dihydrofolate reductase: Crystallographic evidence. Biochemistry 36: 586−603.

Schlick T, Li B, Olson WK (1994) The influence of salt on the structure and energetics of supercoiled DNA. Biophys. J. 67: 2146−2166.

Schnell JR, Dyson HJ, Wright PE (2004) Structure, dynamics, and catalytic function of dihydrofolate reductase. Annu. Rev. Biophys. Biomol. Struct. 33: 119−140.

Sinha R, Khare SK (2014) Protective role of salt in catalysis and maintaining structure of halophilic proteins against denaturation. Front. Microbiol. 5:165. doi: 10.3389/fmicb.2014.00165.

Stone SR, Morrision JF (1982) Kinetic mechanism of the reaction catalyzed by dihydrofolate reductase from *Escherichia coli*. Biochemistry 21: 3757−3765.

Takashina T, Hamamoto T, Otozai K, Grant WD, Horikoshi K (1990) *Haloarcula japonica* sp. nov., a new triangular halophilic archaebacterium. System. Appl. Microbiol. 13: 177−181.

Takashina T, Otozati K, Hamamoto T, Horikoshi K (1994) Isolation of halophilic and halotolerant bacteria from a Japanese salt field and comparison of the partial 16S rRNA gene sequence of an extremely halophilic isolate with those of other extreme halophiles. Biodiversity and Conservation 3: 632−642.

Viola RE, Cook PF, Cleland WW (1979) Stereoselective preperration of deuterated reduced nicotinamide adenine dinucleotide and substrates by enzymatic synthesis. Anal. Biochem. 96:334–340.

Wakai S, Kidokoro S, Masaki K, Nakasone K, Sambongi Y (2013) Constant enthalpy change value during pyrophosphate hydrolysis within the physiological limits of NaCl. J. Biol. Chem. 288: 29247−29251.

Wang Z, Singh P, Czekster CM, Kohen A, Schramm VL (2014 Protein mass-modulated effects in the catalytic mechanism of dihydrofolate reductase: Beyond promoting

vibration. J. Am. Chem. Soc. 136: 8333–8341.

Williams JW, Morrison JF, Duggleby RG (1979) Methotrexate, a high-affinity pseudosubstrate of dihydrofolate reductase. Biochemistry 18:2567–2573.

Woody RW (1977) Optical rotatory properties of biopolymers. J. Polym. Sci. Part D: Macromol. Rev. 12: 181−320.

Wright DB, Banks DD, Lohman JR, Hilsenbeck JL, Gloss LM (2002) The effect of salts on the activity and stability of *Escherichia coli* and *Haloferax volcanii* dihydrofolate reductases. J. Mol. Biol. 323: 327−344.

Zusman T, Rosenshine I, Boehm G, Jaenicke R, Leskiw B, Mevarech M (1989) Dihydrofolate reductase of the extremely halophilic archaebacterium *Halobacterium volcanii*. J. Biol. Chem. 264: 18878−18883.

Acknowledgements

I acknowledge to Assoc. prof. K. Katayanagi for patient supervising, to Assist. prof. E. Ohmae for teaching experimental methods, giving useful comments, and much discussions about this study, and to Prof. S. Tate, Assoc. prof. N. Tochio, and Assist. prof. F. Holger for teaching experimental methods and fruitful discussions about this study. I am grateful to Prof. K. Nakasone for the gift of genomic DNA from *H. japonica* strain TR-1, to Ms. T. Amimoto, Natural Science Center for Basic Research and Development of Hiroshima University for the use and technical assistance of ESI-MS apparatus, and to Prof. N. Ito and Assoc. prof. T. Ikura for the use of stopped-flow apparatus and discussions about this study. I am thankful to Prof. S. Izumi, Prof. K. Gekko, Prof. Y. Sambongi, Prof. M. Aida, and Prof. S. Nakata for reviewing this thesis. I would like to say thank all of laboratory members for teaching basic experimental methods and cheering up when I was in trouble.

This work was supported financially by a JSPS KAKENHI Grant (No. 24570186 to E. Ohmae.), a Sasagawa Scientific Research Grant from the Japan Science Society (No. 26-315 to Y. Miyashita.), the Hiroshima University Education and Research Support Foundation, and the Platform Project for Supporting in Drug Discovery and Life Science Research (Platform for Dynamic Approaches to Living System) from Japan Agency for Medical Research and Development (AMED).

Lastly, I would like to say thank my family for giving encouragement and extremely enormous supports during 27 years. Without their supports, this research would not have been completed.